Partial Modulation Injection for Gas Chromatography

Derrick V. Gough

A thesis

submitted in partial fulfillment of the

requirements for the degree of

Master of Science

University of Washington

2019

Committee:

Robert E. Synovec

Frantisek Turecek

Program Authorized to Offer Degree:

Chemistry

University of Washington

Abstract

Partial Modulation Injection for Gas Chromatography

Derrick V. Gough

Chair of the Supervisory Committee:
Professor Robert E. Synovec
Department of Chemistry

Partial modulation is developed and refined for one-dimensional gas chromatography (1D-GC), comprehensive two-dimensional gas chromatography (GC×GC), and comprehensive three-dimensional gas chromatography (GC^3). Since it's first inception, partial modulation as a technique has been relatively unstudied. In partial modulation, a small segment of the analyte concentration profile is modulated, where the first dimension, ^1D, peak profile is retained while superimposing the second dimension, ^2D, separation profile on top. The pulse flow valve modulator, operating in partial modulation modes, enables a large increase in chemical information density, that is the same chemical separation, or peak capacity, that is possible with current modulators can be done in a fraction (as low as every 50 ms vs > 250 ms) of the time. Coupling this modulator to an optimized GC×GC instrument provides an optimized GC^3 instrument that can physically separate up to ~31,000 peaks in a 40 min separation, or a total of ~770 peaks separated

per minute of separation run time. Additionally, the pulse flow valve can operate as an injector to a 1D-GC instrument, where it can separate similar, volatile organic compounds in very short time periods (demonstrated at 200 ms and 500 ms) with baseline resolution between all analytes. This modulation technique has readily provided analyte w_b as narrow as single-digit ms, affording incredibly high peak capacities in very short modulation periods. The application of the pulse flow valve modulator, operated in the relatively un-studied partial modulation modes, has demonstrated the ability to greatly increase the physical separation between analytes in complex mixtures, which in turn can increase the scope and applicability of GC instrumentation.

TABLE OF CONTENTS

LIST OF FIGURES

Page

LIST OF TABLES

Page

ACKNOWLEDGEMENTS

I wish to express my most sincere gratitude to all the current and former members of the Synovec Group during my brief tenure at the University of Washington – none of this would have been possible without your support. You are all amazing scientists, brilliant researchers, and wonderful people. I am excited to see where each of you go from here. “We can resolve that.”

It has truly been a privilege to research underneath Professor Rob Synovec. Having come into this field completely unaware of the existence of multidimensional gas chromatography, I am truly blown away by how much you have taught me, and how you are, incredibly, always right. I have grown exponentially as a person and researcher thanks to your mentorship. I could never have been this successful without your guidance and instruction.

To Abby, thank you again for joining me in this latest adventure. I wouldn’t be here if you weren’t there with me over the past 11 years. I can never thank you enough for your constant support of me through these many endeavors.

DEDICATION

To my wife, Abby. You always bring out the best in me and are my constant source of inspiration.

Words will never be enough to convey my love for you.

Chapter 1. Introduction to Multidimensional Gas Chromatography.

1.1 INTRODUCTION

Gas chromatography (GC) is a powerful analytical technique that can separate, identify, and quantify volatile and semi-volatile analytes. Despite the efficiency and separation power of a one-dimensional (1D) GC, complex mixtures of similar compounds (such as petroleum products or metabolites) cannot always be sufficiently resolved or separated. In 1991 [1], Lui and Phillips experimentally pioneered a form of multidimensional GC (MDGC) known as comprehensive two-dimensional (2D) gas chromatography (GC×GC). The addition of a second separation dimension (i.e. column one with a nonpolar and column two with a polar stationary phase) provides a complementary separation and has greatly increased the separating and resolving power of GC-based separation methods [2–5]. Now, analytes that are overlapped on the first dimension (^{1}D) can be resolved on the second dimension (^{2}D), enabling more complete separations of complex mixtures [6–9].

The heart of the GC×GC instrument is the modulator, which transfers the effluent from the 1D separation to a comprehensive 2D separation. Generally, GC×GC instruments rely upon "full" modulation methods, where all of the analyte is modulated and separated [10]. During full modulation, the entire analyte is compressed into a pulse, focused, reinjected and further separated on a second column. This is the case whether a modulator transfers 100% of the eluate (duty cycle = 1.0), or if it transfers only a fraction of the eluate (duty cycle < 1.0). With some data processing, the original shape and pertinent ^{1}D figures-of-merit (such as peak width-at-base, W_b, and retention time, t_r) can be obtained. Central to MDGC are the concepts of sampling

density and peak capacity. Sampling density, ρ_s, is defined as the number of modulations per ^{1}D analyte peak.

$$\rho_s = \frac{^1W_b}{P_M} \tag{1.1}$$

For a comprehensive separation, ρ_s ideally is between 2 and 4, ensuring proper sampling of the previous dimension without oversampling an excessively wide peak [11–13].

When compared to 1D-GC, GC×GC theoretically provides a 10-fold improvement in peak capacity (n_c) [14–17] due to the second dimension. In our research, the best practice of GC×GC relies on maximizing peak capacity. The 1D separation peak capacity (n_c), at unit resolution, R_s = 1, is defined as the total time (^1t) of the ^{1}D separation divided by the average width-of-base, ^1W_b, of the analytes

$$n_c = \frac{^1t}{^1W_b} \tag{1.2}$$

For GC×GC the ideal peak capacity is given by,

$$n_{c,2D} = {}^1n_c \times {}^2n_c \tag{1.3}$$

where ^1n_c and ^2n_c are the ^{1}D and ^{2}D peak capacities, respectively. Equation (1.3) can be expanded in terms of modulator performance, and the impact on peak capacity optimization,

$$n_{c,2D} = \frac{^1t}{^1W_b} \times \frac{^2t}{^2W_b} = \frac{^1t}{^1W_b} \times \frac{P_M}{^2W_b} \tag{1.4}$$

Similar to the leap from 1D-GC to GC×GC, we have recently begun exploring the jump to comprehensive three-dimensional GC, referred to as GC^3, to further increase separation power and enhance chemical selectivity [18–23]. One then imagines a similar improvement in peak capacity when moving from GC×GC to GC^3. However, this was not possible in early studies, as there was no modulator available that could be used fast enough to not “dummy-down,” or

artificially widen, the previous 2 dimensions. Early GC^3 instruments traded total peak capacity for increased selectivity in the third dimension (^3D) [19], where the ^3D was used like a multivariate detector [20]. Initially, the GC^3 instrument could only obtain a peak capacity ($n_{c,3D}$) comparable to, albeit lower than, optimized GC×GC instruments [19,20]. While promising, the initial instruments did not have the same separating power as current GC×GC instruments [5,14,24–26], as modulators were not sufficiently fast enough (i.e. modulation period, P_M, is too long) to modulate ^2D peaks effectively. More recent work using partial modulation methods have shown that the GC^3 instrument can reach peak capacities approaching 10,000 in 11 min [23].

The GC^3 instrument has the potential to be very useful for the analysis of complex samples. However, there remains a need to provide more peak capacity coupled with more effective use of the separation space. To address this challenge, we explored the manipulation of phase volume ratios, β, [27] to further optimize the GC^3 instrument. The β for an open tubular capillary column is the ratio of the volume of the mobile phase, V_m, to the volume of the stationary phase, V_s,

$$\beta = \frac{Vm}{Vs} = \frac{d_c}{4d_f} \tag{1.5}$$

where d_c is the capillary column's inner diameter and d_f is the stationary phase's film thickness. The phase volume ratio β is immensely important for GC, as it is directly related to the retention factor, k. Manipulating β through the selection of columns with different d_c and d_f enables modification of analytes' elution temperatures, T_e [28]. For GC×GC separations, it has been recently reported that one can more effectively control and improve the *useful* peak capacity by considering the β_r, the ratio of β between dimensions [27]

$$^x\beta_r = \frac{^x\beta}{^{x+1}\beta} \tag{1.6}$$

Prudent selection of the β_r of a GC×GC system improved peak capacity and the use of the available separation space. A positive linear dependence between ${}^2W_b$ and ${}^2k$ was demonstrated, and shown to be independent of ${}^1t_r$ [27]. Additionally, increasing β_r will also increase ${}^2k$, and therefore plays a pivotal role in the peak capacity of the separation [27]. Lessons learned from this previous GC×GC study are directly applicable to improving GC^3 instrumentation for addressing current goals. Additional discussion concerning the effect of the β_r on MDGC can be found in previous reports [25,27].

1.2 Challenges And Motivations

Gas chromatography is a well-established, mature field for analysis. As such, it is constantly given more complex mixtures (such as diesels and metabolic samples) with tens of thousands of components which may never be fully resolved. One approach to handle such complex mixtures is the proper application of chemometric techniques. While there are no one-size fits all technique, chemometric analysis has proven itself invaluable in both targeted and un-targeted analysis. Despite the number of chemometric techniques available, they all fail after a separation is too saturated and there are too many components co-eluting. This can be dealt with by using a modulator, or modulation technique, that provides improved separating capability before the data every gets to the analyst. Improvements in total peak capacity, regardless of the detector, can enable current chemometric techniques to perform better and improve the extraction of useful chemical information.

Modulator technology has evolved a great deal since its inception nearly 30 years ago. Thermal and flow-based modulators provide incredible improvements (in resolving power and peak capacity) to a 1D-GC separation. However, neither are without flaws. Thermal modulators typically require expensive and resource intensive (lab space) cryogenic fluids. While a push

continues for improved cryogen-free thermal modulators, there will always be breakthrough concerns for low boiling point analytes, and a lack of ability to properly modulate very heavy analytes as well. Flow-based modulators address these shortcomings but are often unable to sample the entire 1D effluent, thus losing overall *S/N* (as not all of an analyte makes it to the detector). Additionally, flow-based modulators often operate at very high flow rates, meaning additional considerations, such as column splitting, are required before attachment to a mass spectrometer. Additionally, neither form of modulator can modulate below 250 ms, leaving a gaping hole in fast GC analysis.

With these challenges in mind, the research presented herein demonstrates our efforts to improve gas-phase separations in 1D-GC, GC×GC, and GC^3. Chapter 2 builds upon the work first pioneered by Cai and Stearns [10], later re-introduced by Freye et al. [29], and then combines it with a theoretical study by Parsons et al. [27]. The application of a new, ultrafast modulator combined with a new strategy for appropriate selection of column dimensions for multidimensional GC was done to show the true separating power of an optimized GC^3 instrument over a traditional-length GC separation. It is hypothesized that the application of this new variable, the ratio of phase volume ratios, will enable tight control of ^2k' and ^3k' throughout a separation, enabling a peak capacity production nearing 1,000 peaks/min to be achieved regardless of the separation time frame.

Chapter 3 aims to develop upon an un-studied method of partial modulation, termed the negative pulse mode by its original pioneers, Cai and Stearns [10]. Previous reports by our group [23,29,30] have solely focused on only the positive pulse mode, which, while effective, creates unwanted preprocessing steps in order to extract the pertinent chemical information from the raw data. The negative pulse mode will produce positive peaks, and it is hypothesized that these peaks

will retain many of the same impressive figures-of-merit (narrow, reproducible w_b, high resolution between volatile compounds) while simultaneously reducing the number of preprocessing steps for the extraction of chemical information.

1.3 REFERENCES

[1] Z. Liu, J.B. Phillips, Comprehensive two-dimensional gas chromatography using an on-column thermal modulator interface, J. Chromatogr. Sci. 29 (1991) 227–231. doi:10.1093/chromsci/29.6.227.

[2] H.D. Bean, J.-M.D. Dimandja, J.E. Hill, Bacterial volatile discovery using solid phase microextraction and comprehensive two-dimensional gas chromatography–time-of-flight mass spectrometry, J. Chromatogr. B. 901 (2012) 41–46. doi:10.1016/j.jchromb.2012.05.038.

[3] S. Prebihalo, A. Brockman, J. Cochran, F.L. Dorman, Determination of emerging contaminants in wastewater utilizing comprehensive two-dimensional gas-chromatography coupled with time-of-flight mass spectrometry, J. Chromatogr. A. 1419 (2015) 109–115. doi:10.1016/j.chroma.2015.09.080.

[4] P.-H. Stefanuto, K.A. Perrault, L.M. Dubois, B. L'Homme, C. Allen, C. Loughnane, N. Ochiai, J.-F. Focant, Advanced method optimization for volatile aroma profiling of beer using two-dimensional gas chromatography time-of-flight mass spectrometry, J. Chromatogr. A. 1507 (2017) 45–52. doi:10.1016/j.chroma.2017.05.064.

[5] L.M. Dubois, K.A. Perrault, P.-H. Stefanuto, S. Koschinski, M. Edwards, L. McGregor, J.-F. Focant, Thermal desorption comprehensive two-dimensional gas chromatography coupled to variable-energy electron ionization time-of-flight mass spectrometry for monitoring subtle changes in volatile organic compound profiles of human blood, J. Chromatogr. A. 1501 (2017) 117–127. doi:10.1016/j.chroma.2017.04.026.

[6] C.E. Freye, B.D. Fitz, M.C. Billingsley, R.E. Synovec, Partial least squares analysis of rocket propulsion fuel data using diaphragm valve-based comprehensive two-dimensional gas chromatography coupled with flame ionization detection, Talanta. 153 (2016) 203–210. doi:10.1016/j.talanta.2016.03.016.

[7] P. Dimitriou-Christidis, A. Bonvin, S. Samanipour, J. Hollender, R. Rutler, J. Westphale, J. Gros, J.S. Arey, GC×GC quantification of priority and emerging nonpolar halogenated micropollutants in all types of wastewater matrices: Analysis methodology, chemical occurrence, and partitioning, Environ. Sci. Technol. 49 (2015) 7914–7925. doi:10.1021/es5049122.

[8] D. Megson, R. Kalin, P.J. Worsfold, C. Gauchotte-Lindsay, D.G. Patterson, M.C. Lohan, S. Comber, T.A. Brown, G. O'Sullivan, Fingerprinting polychlorinated biphenyls in environmental samples using comprehensive two-dimensional gas chromatography with time-of-flight mass spectrometry, J. Chromatogr. A. 1318 (2013) 276–283. doi:10.1016/j.chroma.2013.10.016.

[9] J.E. Welke, V. Manfroi, M. Zanus, M. Lazzarotto, C. Alcaraz Zini, Differentiation of wines according to grape variety using multivariate analysis of comprehensive two-

dimensional gas chromatography with time-of-flight mass spectrometric detection data, Food Chem. 141 (2013) 3897–3905. doi:10.1016/j.foodchem.2013.06.100.
[10] H. Cai, S.D. Stearns, Partial modulation method via pulsed flow modulator for comprehensive two-dimensional gas chromatography, Anal. Chem. 76 (2004) 6064–6076. doi:10.1021/ac0492463.
[11] L.M. Blumberg, Accumulating resampling (modulation) in comprehensive two-dimensional capillary GC (GC×GC), J. Sep. Sci. 31 (2008) 3358–3365. doi:10.1002/jssc.200800424.
[12] W. Khummueng, J. Harynuk, P.J. Marriott, Modulation ratio in comprehensive two-dimensional gas chromatography, Anal. Chem. 78 (2006) 4578–4587. doi:10.1021/ac052270b.
[13] W.C. Siegler, B.D. Fitz, J.C. Hoggard, R.E. Synovec, Experimental study of the quantitative precision for valve-based comprehensive two-dimensional gas chromatography, Anal. Chem. 83 (2011) 5190–5196. doi:10.1021/ac200302b.
[14] M.S. Klee, J. Cochran, M. Merrick, L.M. Blumberg, Evaluation of conditions of comprehensive two-dimensional gas chromatography that yield a near-theoretical maximum in peak capacity gain, J. Chromatogr. A. 1383 (2015) 151–159. doi:10.1016/j.chroma.2015.01.031.
[15] J.M. Davis, Statistical theory of spot overlap for n-dimensional separations, Anal. Chem. 65 (1993) 2014–2023. doi:10.1021/ac00063a015.
[16] J.M. Davis, J.Calvin. Giddings, Statistical theory of component overlap in multicomponent chromatograms, Anal. Chem. 55 (1983) 418–424. doi:10.1021/ac00254a003.
[17] J.M. Davis, J.Calvin. Giddings, Statistical method for estimation of number of components from single complex chromatograms: theory, computer-based testing, and analysis of errors, Anal. Chem. 57 (1985) 2168–2177. doi:10.1021/ac00289a002.
[18] D. Chen, J.H. Seo, J. Liu, K. Kurabayashi, X. Fan, Smart three-dimensional gas chromatography, Anal. Chem. 85 (2013) 6871–6875. doi:10.1021/ac401152v.
[19] N.E. Watson, W.C. Siegler, J.C. Hoggard, R.E. Synovec, Comprehensive three-dimensional gas chromatography with parallel factor analysis, Anal. Chem. 79 (2007) 8270–8280. doi:10.1021/ac070829x.
[20] W.C. Siegler, J.A. Crank, D.W. Armstrong, R.E. Synovec, Increasing selectivity in comprehensive three-dimensional gas chromatography via an ionic liquid stationary phase column in one dimension, J. Chromatogr. A. 1217 (2010) 3144–3149. doi:10.1016/j.chroma.2010.02.082.
[21] N.E. Watson, H.D. Bahaghighat, K. Cui, R.E. Synovec, Comprehensive three-dimensional gas chromatography with time-of-flight mass spectrometry, Anal. Chem. 89 (2017) 1793–1800. doi:10.1021/acs.analchem.6b04112.
[22] N.E. Watson, S.E. Prebihalo, R.E. Synovec, Targeted analyte deconvolution and identification by four-way parallel factor analysis using three-dimensional gas chromatography with mass spectrometry data, Anal. Chim. Acta (2017). doi:10.1016/j.aca.2017.06.017.
[23] H.D. Bahaghighat, C.E. Freye, D.V. Gough, P.E. Sudol, R.E. Synovec, Ultrafast separations via pulse flow valve modulation to enable high peak capacity multidimensional gas chromatography, J. Chromatogr. A. (2018). doi:10.1016/j.chroma.2018.08.001.

[24] C.E. Freye, R.E. Synovec, High temperature diaphragm valve-based comprehensive two-dimensional gas chromatography with time-of-flight mass spectrometry, Talanta. 161 (2016) 675–680. doi:10.1016/j.talanta.2016.09.002.
[25] A.M. Muscalu, M. Edwards, T. Górecki, E.J. Reiner, Evaluation of a single-stage consumable-free modulator for comprehensive two-dimensional gas chromatography: Analysis of polychlorinated biphenyls, organochlorine pesticides and chlorobenzenes, Journal of Chromatography A. 1391 (2015) 93–101. doi:10.1016/j.chroma.2015.02.074.
[26] J.V. Seeley, N.E. Schimmel, S.K. Seeley, The multi-mode modulator: A versatile fluidic device for two-dimensional gas chromatography, Journal of Chromatography A. 1536 (2018) 6–15. doi:10.1016/j.chroma.2017.06.030.
[27] B.A. Parsons, D.K. Pinkerton, R.E. Synovec, Implications of phase ratio for maximizing peak capacity in comprehensive two-dimensional gas chromatography time-of-flight mass spectrometry, Journal of Chromatography A. 1536 (2018) 16–26. doi:10.1016/j.chroma.2017.07.018.
[28] L. Mahé, M. Courtiade, C. Dartiguelongue, J. Ponthus, V. Souchon, D. Thiébaut, Overcoming the high-temperature two-dimensional gas chromatography limits to elute heavy compounds, Journal of Chromatography A. 1229 (2012) 298–301. doi:10.1016/j.chroma.2012.01.030.
[29] C.E. Freye, H.D. Bahaghighat, R.E. Synovec, Comprehensive two-dimensional gas chromatography using partial modulation via a pulsed flow valve with a short modulation period, Talanta. 177 (2018) 142–149. doi:10.1016/j.talanta.2017.08.095.
[30] H.D. Bahaghighat, C.E. Freye, D.V. Gough, R.E. Synovec, Comprehensive two-dimensional gas chromatography and time-of-flight mass spectrometry detection with a 50 ms modulation period, Journal of Chromatography A. (2018). doi:10.1016/j.chroma.2018.11.027.

Chapter 2. Column Selection Approach to Achieve a High Peak Capacity in Comprehensive Three-Dimensional Gas Chromatography

This chapter was reproduced from Derrick V. Gough, H. Daniel Bahaghighat, and R.E. Synovec, "Column Selection Approach to Achieve a High Peak Capacity in Comprehensive Three-Dimensional Gas Chromatography" *Talanta* 195 *(*2019) 822-829.

2.1 INTRODUCTION

Gas chromatography (GC) is a powerful analytical technique that can separate, identify, and quantify volatile and semi-volatile analytes. Despite the efficiency and separation power of a traditional one-dimensional (1D) GC, complex mixtures of similar compounds (such as petroleum products or metabolites) cannot always be sufficiently resolved or separated. In 1991 [1], Lui and Phillips experimentally pioneered a form of multidimensional GC (MDGC) known as comprehensive two-dimensional (2D) gas chromatography (GC×GC). The addition of a second separation dimension with a different polarity relative to 1D-GC provides a complementary separation. Indeed, the advent of GC×GC has greatly increased the separating and resolving power of GC-based separation methods [2–5]. Now, analytes that are overlapped on the first dimension (^{1}D) can be resolved on the second dimension (^{2}D), enabling more complete separations of complex mixtures [6–9].

Similar to the leap from 1D-GC to GC×GC, researchers have recently begun exploring the jump to comprehensive three-dimensional GC, referred to as GC^3, in order to further increase separation power and enhance chemical selectivity [10–15]. When compared to 1D-GC, GC×GC theoretically provides roughly a 10-fold improvement in peak capacity [16–19] due to the

addition of the second dimension. It is intriguing to imagine a similar improvement in peak capacity may be gleaned when moving from GC×GC to GC^3, if the instrumental design is carefully considered. However, early studies traded total peak capacity for increased selectivity in the third dimension (^{3}D) [11]. Essentially, the third dimension was used primarily like a multivariate detector, providing an additional form of and/or enhancing the chemical selectivity [12]. In these studies, the GC^3 instrument was able to obtain a peak capacity of 3,500 in 60 min, and then the instrumentation was improved to obtain the same peak capacity in one-third of the time [11,12]. While being very promising, the initial instruments did not have the same level of separation power as current GC×GC instruments [5,16,20–22]. More recent work has shown that the GC^3 instrument is not only able to retain the same separation power [13] as GC×GC, but is now able to improve upon it with peak capacities of up to 10,000 in 11 min, with peak capacity production nearing 1,000 peaks/min [15].

The leap in separating power (i.e. peak capacity and peak capacity production) from state-of-the-art GC×GC to GC^3 instruments was made possible by the evolution of the available modulators that link each successive separation dimension together. Moreover, the modulator is essential in transferring the eluate from the previous to successive separation dimension at a user-defined time interval, known as the modulation period, P_M. There are two broad categories of modulators: thermal [23–26] and flow-based [27–31] modulators. Briefly, thermal modulators use a thermal means of focusing (often with cryogenics) to trap analytes and then a rapid heating mechanism to quickly desorb, or reinject, the analytes onto a subsequent column. There are three general types of thermal modulators: resistively heated trap [1,32], heated sweeper [33,34], and cryogenic focus [25,35,36]. Flow-based modulators isolate the eluate coming from a given column into a sample loop at the modulator. An auxiliary carrier gas flow

periodically compresses and reinjects the analytes onto the subsequent column. This auxiliary carrier gas flow is independently controlled, and for example with GC×GC, is often much higher than the flow through the ^{1}D column [20,27,29,37]. Thermal modulators have the benefit of a duty cycle of 1.0 (or zero loss of analyte between dimensions) with the added issues that come with more equipment to trap and rapidly reheat analytes. Flow-based modulators, which are still able to provide comprehensive sampling between successive separation dimensions, typically have a duty cycle less than 1.0 (i.e. some loss of analyte at the modulator) but are generally less equipment intensive and simpler to operate [38].

Herein, we refer to these types of modulators as providing "full" modulation, as the entirety of the analyte concentration profile for a given time interval is modulated each time the modulator actuates [39]. During full modulation, the analyte is trapped and/or compressed into a pulse that is then introduced to the subsequent separation column for separation from concurrently modulated analytes. Albeit with some data processing, for example with GC×GC, the original shape and pertinent ^{1}D figures-of-merit (such as peak width-at-base, W, and retention time, t_r) can be obtained. In contrast to full modulation, a relatively unexplored modulation approach pioneered by Cai and Sterns is referred to as "partial" modulation, with more recent reports by our group [15,39,40]. Relative to full modulation, during partial modulation a distinct fraction of the analyte concentration profile within a given time interval is modulated, enabling the original peak shape to be retained with additional chromatographically-encoded chemical information within each partial modulation. Indeed, most recently, the use of a pulse flow valve modulator to perform partial modulation enabled researchers to analyze and interpret this encoded information by using the properties of vacancy chromatography and frontal analysis [15,40,41]. Moreover, the pulse flow valve modulator can operate with an ultrafast P_M, as low as

50 ms [15]. This ultrafast modulator is ideally suited as the second modulator in a GC^3 instrument, enabling researchers to not sacrifice optimum separation conditions on the ^{1}D and ^{2}D columns, concurrent with effective and efficient modulation onto the ^{3}D column [15].

The GC^3 instrument has the potential to be very useful for the analysis of complex samples, and building upon this most recent study [15], there remains a need to provide more peak capacity coupled with more effective use of the 3D separation space. To address this challenge, herein we explore the means to further optimize the GC^3 instrument to improve its separating power. A relatively unexplored avenue to increase and to make more effective use of the peak capacity, is the manipulation of *the ratio* of the phase volume ratios, β_r, between successive separation dimensions in GC^3, as previously studied with GC×GC [42]. In the process of doing so, we note that commercial availability of GC columns must be taken into account, as there are relatively limited options of common, commercially available phase volume ratios, β, to choose from for typical GC×GC and emerging GC^3 instrument designs, such as β of 250 (capillary insider diameter d_c of 180 µm with a film thickness d_f of 0.180 µm), 112.5 (d_c: 180 µm, d_f: 0.40 µm), 62.5 (d_c: 250 µm, d_f: 1.0 µm), 625 (d_c: 250 µm, d_f: 0.10 µm), 250 (d_c: 100 µm, d_f: 0.1 µm), 125 (d_c: 100 µm, d_f: 0.2 µm), to list a few. Since our focus is on producing a high peak capacity GC^3 design, we rely upon columns with d_c of 180 and 100 µm.

2.2 FUNDAMENTAL PRINCIPLES

2.2.1 *Beta Ratio*

The phase volume ratio, β, for an individual open tubular capillary column is the ratio of the volume of the mobile phase, V_m, to the volume of the stationary phase, V_s,

$$\beta = \frac{Vm}{Vs} = \frac{d_c}{4d_f} \tag{2.1}$$

where d_c is the inner diameter of the capillary column and d_f is the film thickness of the stationary phase. The phase volume ratio β is immensely important for GC, as it is directly related to the retention factor, k, for each analyte. Manipulating β through the selection of various columns with different d_c and d_f, while keeping the stationary phases constant (or nearly so) has enabled researchers to modify the elution temperature [43], T_e, of analytes and to do phase ratio focusing [44] without changing chemical selectivity.

For GC×GC separations, it has been recently reported that through the selection of appropriate β values between successive dimensions, the analyst can more effectively control and improve the *useful* peak capacity of their GC×GC separations [42]. From this report, the operative variable for this control is the β ratio between successive dimensions, β_r,

$$ {}^{x}\beta_r = \frac{{}^{x}\beta}{{}^{x+1}\beta} \tag{2.2}$$

Hence, prudent selection of the β_r between successive separation dimensions, ^{1}D and ^{2}D, of a GC×GC system, while holding all other separation variables essentially constant, was demonstrated to enable peak capacity and use of the available 2D separation space to be more effectively controlled. The analyst can alter the T_e of an analyte from the ^{1}D column (termed ^1T_e) by modifying its phase ratio, $^1\beta$. Also, since the ^{2}D separation is a short column with a short P_m, typically in the range of a few seconds, the ^{2}D separation is pseudo-isothermal. A positive linear dependence of ^2W on ^2k was demonstrated, and shown to be independent from ^1t_r [42]. Additionally, changing the ^1T_e of an analyte modifies the temperature the analyte experiences on the pseudo-isothermal ^{2}D separation. For instance, decreasing the $^1\beta$ (increasing the d_f to d_c ratio) causes ^1T_e to increase, resulting in the ^{2}D separation occurring at a higher temperature. The same analyte undergoing the same ^{2}D separation at a higher temperature will demonstrate a lower ^2k than at a lower temperature. Proper selection of the ^{2}D phase volume ratio, $^2\beta$, gives effective

control of analyte retention on ^{2}D. Overall, β_r conveniently describes the relative k on successive separation dimensions; increasing β_r will also increase ^2k, and therefore plays a pivotal role in maximizing the peak capacity of the overall separation [42]. Additionally, β_r affects the potential ^2k range for analytes; a lower β_r allows for a lower starting ^2k, while a higher β_r allows for a larger range of ^2k. Lessons learned from this GC×GC study using β_r to control performance appear to be directly applicable to improving GC^3 column selection for addressing the need to increase GC^3 peak capacity, as is presented herein.

2.2.2 *Peak Capacity*

In this study, we do not take into account geometrical, statistical, and column set orthogonality considerations for peak capacity [17,45–47] since their effect has not been sufficiently developed for GC^3. Instead, we make comparisons using an expression for ideal peak capacity as defined by Giddings [48], which is simply the product of the peak capacity for each dimension. This provides clarity and consistency with our previous GC^3 work. A discussion of GC^3 peak capacity begins in the context of a given 1D separation dimension, x, at unit resolution, $R_s = 1$, defined as the separation time, t, which is the portion of the total separation used to determine peak capacity, $^x n_c$, divided by the average width-at-base (4σ), W,

$$^x n_c = \frac{^x t}{^x W} \tag{2.3}$$

For GC×GC, or for two coupled columns in GC^3, the ideal peak capacity is given by,

$$n_{c,2D} = {}^x n_c \, {}^{x+1} n_c \tag{2.4}$$

where $^x n_c$ and $^{x+1} n_c$ are the peak capacities of the two successive separations, specifically $^1 n_c \times {}^2 n_c$ in GC×GC, or $^1 n_c \times {}^2 n_c$ and $^2 n_c \times {}^3 n_c$ in GC^3. Based upon Eqs. (2.3) and (2.4), for GC^3, the ideal peak capacity is given by,

$$n_{c,3D} = {}^{1}n_c\,{}^{2}n_c\,{}^{3}n_c \tag{2.5}$$

At unit resolution, Eq. (2.5) can be expressed as,

$$n_{c,3D} = \frac{{}^{1}t}{{}^{1}W}\frac{{}^{1}P_{\mathrm{M}}}{{}^{2}W}\frac{{}^{2}P_{\mathrm{M}}}{{}^{3}W} \tag{2.6}$$

where ${}^{1}t$ is the portion of the total run time on ^{1}D used to determine the peak capacity, and ${}^{1}P_{\mathrm{M}}$ and ${}^{2}P_{\mathrm{M}}$ are the first and second modulation periods, equal to the ^{2}D run time and ^{3}D run time, respectively. In order for GC×GC and GC^3 separations to be sufficiently comprehensive, the sampling density, ρ_s, should be $\rho_s \geq 2$ [49–51],

$${}^{x}\rho_s = \frac{{}^{x}W}{{}^{x}P_{\mathrm{M}}} \tag{2.7}$$

Combining Eqs. (2.6) and (2.7), one can put $n_{c,3D}$ in terms of the ^{1}D and ^{2}D sampling densities, ${}^{1}\rho_s$ and ${}^{2}\rho_s$, respectively,

$$n_{c,3D} = \frac{1}{{}^{1}\rho_s}\frac{1}{{}^{2}\rho_s}\frac{{}^{1}t}{{}^{3}W} \tag{2.8}$$

Equation (2.8) indicates that to maximize $n_{c,3D}$, the peak width on ^{3}D given by ${}^{3}W$ must be minimized, as well as operating the GC^3 instrument with minimally allowable sampling densities on ^{1}D and ^{2}D. The pulse flow valve modulator has been shown to able to operate at P_{M} of as low as 50 ms and provides very narrow ${}^{3}W$, on the order of 10 ms [15,40]. The ${}^{1}\rho_s$ can be minimized by proper chromatographic conditions to control the ${}^{1}W$, such as temperature programming rates for GC. The ${}^{2}\rho_s$ can be minimized by controlling the ${}^{1}\beta_r$ selected. As recently demonstrated, a lower ${}^{1}\beta_r$ equates to lower ${}^{2}k$ values and ${}^{2}W$ [42] across the entire separation. Moreover, the lower ${}^{1}\beta_r$ properly reduces the range of possible ${}^{2}k$ values, enabling us to keep the range of ${}^{2}W$ manageable to achieve a proper ${}^{2}\rho_s$. Indeed, the results reported in this previous study of the impact of β_r in GC×GC [42] serves as a control experiment indicating that a $\beta_r \sim 0.5$ is well suited for the ^{1}D to ^{2}D dimensions in GC^3.

Learning from our previous GC^3 and β_r studies [15,42], which served as our baseline for the performance of the column selection strategy in GC^3, we now realize that the β_r used to link the ^{1}D and ^{2}D, and ^{2}D and ^{3}D were previously both 1.0 [15] and the β_r of 1.0 for ^{1}D to ^{2}D generally requires an inordinately high ^1P_M [42], which we sought to avoid in the current optimization effort, in order to increase the overall peak capacity, $n_{c,3D}$. However, the noted gain in instrument performance over previous studies [15] came from improvements to the modulator itself, specifically the implementation of the pulse flow valve modulator did produce very narrow ^3W, and did allow some improvements to the ^{1}D and ^{2}D separations while still providing a sufficient $^2\rho_s$. Building from this previous work, we desired to achieve this high level of peak capacity production, but for a longer run time on ^{1}D, to achieve perhaps an ideal $n_{c,3D}$ approaching 40,000, based on Eq. (2.8) for a 40 min run using $^1\rho_s$ and $^2\rho_s$ of ~ 2.5, and achieving ^3W ~ 10 ms. This gain in peak capacity would be roughly 10-fold more than typically achieved in the same time frame with commercial GC×GC instruments. The independence of the relationship of the ^2W to the ^2k from the ^1t_r implied that this is achievable. To achieve this, three goals must be met. First, maximization of the ^{3}D peak capacity, ^3n_c, is required. Second, the ^2P_M and ^3W must be made as small and narrow, respectively, as possible. Third, we seek to achieve a product of the peak capacities for the ^{2}D and ^{3}D separations, $^2n_c \times {}^3n_c$, in the range of ~ 50 to 100, so as to be substantially larger than the value of the typical ^2n_c obtained with GC×GC, which is in the range of ~ 10 to 20 [16]. This last goal is important to bring the total peak capacity production close to 1000 peaks/min as in the previous report. Accordingly, herein we demonstrate that proper selection of β_r between the ^{1}D and ^{2}D separations, specifically a $^1\beta_r$ ~ 0.5 based upon the previous β_r study with GC×GC [42], and the β_r between the ^{2}D and ^{3}D separations, specifically a $^2\beta_r$ ~ 1.0 based upon the prior GC^3 study [15], will enable each of these goals to be concurrently achieved and

sustained over an extended separation time due to the control of the ^{2}k and ^{3}k ranges, coupled with a suitable $^{1}P_{M}$ between ^{1}D and ^{2}D of 2 s to properly sample the peaks eluting from ^{1}D, and a very short $^{2}P_{M}$ between ^{2}D and ^{3}D of 100 ms so the narrow peaks eluting from ^{2}D are properly sampled onto ^{3}D. The resulting data structure is depicted in Fig. 2.1, in which every 2 s along the ^{1}D separation, a GC×GC chromatogram is collected by the ^{2}D × ^{3}D column set with a very high peak capacity for $^{2}n_{c} \times {}^{3}n_{c}$ in the range of ~ 50 to 100 for each modulation of a 40 min ^{1}D separation.

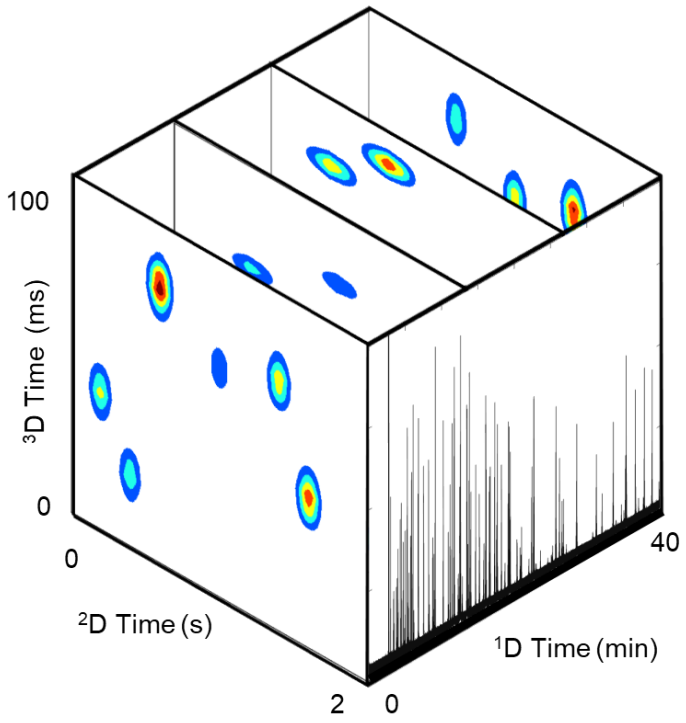

Figure 2.1 Visualization of three-dimensional (3D) data sets from the GC^{3} instrument. There is inherent complexity to visualizing how individual and groups of analytes elute in three distinct time frames on the GC^{3}, and it becomes convenient to consider only the ^{2}D × ^{3}D chromatogram at various points in time along the ^{1}D axis. With a modulation period of 2 s from ^{1}D to ^{2}D, every 2 s along the ^{1}D axis, the GC^{3} instrument reported herein produces a GC×GC chromatogram with an ideal peak capacity in the range of ~ 50 to 100, enabling a large volume of chemical information to be retained and deciphered by the researcher.

2.3 EXPERIMENTAL

The GC^3 instrument, as depicted in Fig. 2.2, was based upon an Agilent 6890 GC (Agilent Technologies, Palo Alto, CA, USA) platform, using a flame ionization detector (FID). The stock electrometer for the Agilent FID was replaced with a high-speed electrometer, built in-house, allowing the data to be collected at 100 kHz, with the data boxcar averaged to 1 kHz. The electrometer was interfaced to a data acquisition board, and the resulting data was collected using an in-house written LabVIEW program (National Instruments, Austin, TX, USA). Post-run data processing was performed in MATLAB R2017b (The Mathworks, Inc., Natick, MA, USA). Samples were introduced to the instrument via a 7683B auto-injector (Agilent Technologies, Palo Alto, CA, USA). Prior to each sample injection, HPLC-grade acetone (Fisher Scientific, Hampton, NH, USA) was used as a solvent rinse. Ultra-high purity hydrogen (Grade 5, 99.999%) was used as the carrier gas (Praxair, Seattle, WA, USA). All experiments utilized an inlet temperature of 175 °C and FID temperature of 250 °C.

The GC^3 instrument was fitted with two modulators: a high-speed, six-port, high-temperature diaphragm valve (VICI model DV12-1116T, Valco Instruments Company Inc., Houston, TX, USA), and a high-speed pulse flow valve (Model 009-0347-900, Parker Hannifin, Hollis, NH, USA). The diaphragm valve was fitted with a 5 µl sample loop, mounted in the oven, linking the ^{1}D and ^{2}D columns. The pulse flow valve, mounted outside the oven, linking the ^{2}D and ^{3}D columns through a 3-way T-union (Model MT.5CXS6, Valco Instruments Company Inc., Houston, TX, USA) mounted inside the oven. An in-house fitting was fabricated to mate the pulse flow valve to 7.24 cm × 1.65 mm copper tubing (Restek, Bellefonte, PA, USA) reduced to 3.81 cm × 0.635 mm steel tubing interfaced with a 2 µl sample loop (Model CSL2, Valco Instruments

Company Inc.) which was connected to the 3-way T-union. The diaphragm valve, pulse flow valve, and the FID were controlled using the same LabView program.

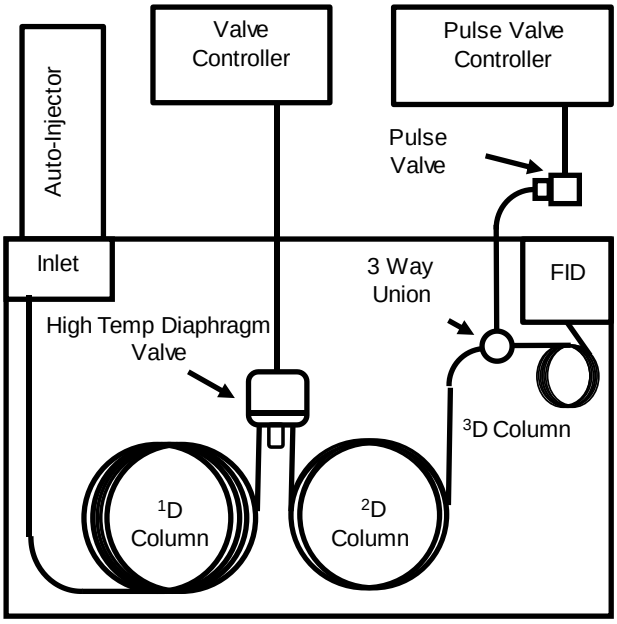

Figure 2.2 Schematic of the main components of the GC^3-FID instrument. The first modulator, linking the ^{1}D and ^{2}D columns was a high-temperature diaphragm valve. The second modulator, linking the ^{2}D and ^{3}D columns was a pulse flow valve.

The ^{1}D column was coated with an RTX-5 Sil MS (5% phenyl/95% dimethylpolysiloxane) stationary phase: 40 m length × 180 µm ^1d_c × 0.40 µm ^1d_f, the ^{2}D column was coated with a DB-17 (50% phenyl/50% dimethylpolysiloxane) stationary phase: 3 m length × 100 µm ^2d_c × 0.1 µm ^2d_f, and the ^{3}D column was coated with a DB-WAX (polyethylene glycol) stationary phase: 0.5 m length × 100 µm ^3d_c × 0.1 µm ^3d_f. Table 2.1 provides a summary for the columns selected. A 2.0 µl volume of a 115-component test mixture was injected at a split of 50:1. The test mixture contained a diverse set of compounds in order to evaluate the instrument setup. The test mixture contained a wide range of boiling points (36–372 °C) with

nine chemical compound classes: alkanes, esters, halogenated alkanes, aromatics, alkenes, alkynes, ketones, alcohols, cycloalkanes [13,40].

	Column 1	Column 2	Column 3
Inner Diameter (d_c), μm	180	100	100
Film Thickness (d_f), μm	0.40	0.10	0.10
Phase Ratio, β	112.5	250	250

Table 2.1 Relevant dimensions for calculating the phase ratio, β, and beta ratio, β_r, of each dimension in the GC^3 instrument. Using Eqs. (2.1) and (2.2), the ${}^1\beta_r$ and ${}^2\beta_r$ can be calculated to be 0.45 and 1.0, respectively.

All three columns were in the same oven, so were subjected to the same temperature at any given time. The oven was set to two temperature program rates, an initial temperature of 40 °C was held for 2.5 min, then ramped at 4.25 °C/min to 164 °C, then immediately ramped 10 °C/min to 240 °C and held for 1 min, for a total run time of 40 min. A programmed flow rate was also used to minimize the general elution problem on the ^{1}D separation, beginning at 1.0 ml/min, ramped by 0.05 ml/min to 2.0 ml/min, then ramped by 0.06 ml/min to 3.2 ml/min. The ^{2}D column flow was controlled via an auxiliary pressure controller with a pressure of 367.5 kPa (53.3 psi), corresponding to a flow rate of 4.5 ml/min. This flow rate was maintained by applying a pressure ramp rate corresponding to the oven temperature to maintain the flow rate of 4.5 ml/min. The ^{3}D column pressure was kept slightly lower than the ^{2}D pressure, 326 kPa (47.3 psi), and ramped concurrently with the ^{2}D column flow. All pressure and flow ramp rates were synchronized with the oven temperature ramp rate. A ${}^1P_M$ of 2 s with an injection pulse width, ${}^1p_w$, of 80 ms was

applied to the diaphragm valve (coupling ^{1}D to ^{2}D), and a ^2P_M of 100 ms with an injection pulse width, ^2p_w, of 2 ms was applied to the pulse flow valve (coupling ^{2}D to ^{3}D).

2.4 Results And Discussion

2.4.1 *Beta Ratio Selection and Data Interpretation*

Table 2.1 summarizes the pertinent dimensions and β's for the three columns selected for the GC^3 instrument. From these β's, per Eq. (2.2), the $^1\beta_r$ (linking the ^{1}D to the ^{2}D) was 0.45 and the $^2\beta_r$ (linking the ^{2}D to the ^{3}D) was 1.0. As previous explained in the Fundamental Principles section, these ratios were selected based on knowledge gained from previous studies [12,13,15,42]. A $^1\beta_r$ of 0.45 was selected to ensure the T_e for analytes eluting from ^{1}D provided a suitable ^2k range on the ^{2}D separation (with ^2n_c in the 5 to 10 range). A relatively shorter ^2k range ensured a very modest range in ^2W as well, enabling the $^2\rho_s$ to remain preferably low throughout the entire run. Additionally, this enabled a modest step down in capillary d_c, with this β_r being easily achievable in a step down of d_c from 250 µm to 180 µm, or 180 µm to 100 µm (which was selected). The overall control of analyte ^2k is prevalent throughout the entire run, which in turn facilitates production of narrow ^2W as will be demonstrated.

Next, with a sufficiently short and efficient column, a $^2\beta_r$ of ~ 1.0 was determined to be appropriate due to the nature of the second modulator. The theory of operation of the pulse flow valve is explained in more detail by Freye et al [40], and the theory of partial modulation is explained more in detail by Cai and Sterns [39]. The same d_c for the ^{2}D and ^{3}D columns ensured the characteristics of the pulse flow valve as a modulator were not interfered with, while minimizing the observance of artifacts within the data. The pulse flow valve can operate at exceptionally fast rates, enabling ultrafast ^2P_M and ^2p_w (operated at 100 ms and 2 ms, respectively). Notably, the same d_c and d_f were used for the ^{3}D and ^{2}D columns, providing a $^2\beta_r$

of 1.0 which also caused the ^{3}D to mimic the pseudo-isothermal nature of the ^{2}D. As importantly, a $^{2}\beta_{r}$ of 1.0 for the ^{2}D × ^{3}D column set has been shown to maximize the peak capacity of the ^{3}D separation in concert with a high peak capacity of the ^{2}D separation, which was a key goal for the development of high peak capacity GC^{3}. No additional consideration to the $^{2}\beta_{r}$, such as control of T_{e} on the ^{2}D dimension, was deemed appropriate. In the context of Eq. (2.8), the current column selection strategy accounts for the $^{1}\rho_{s}$ and $^{2}\rho_{s}$ observed and the pulse flow valve modulator accounts for the narrow ^{3}W achieved.

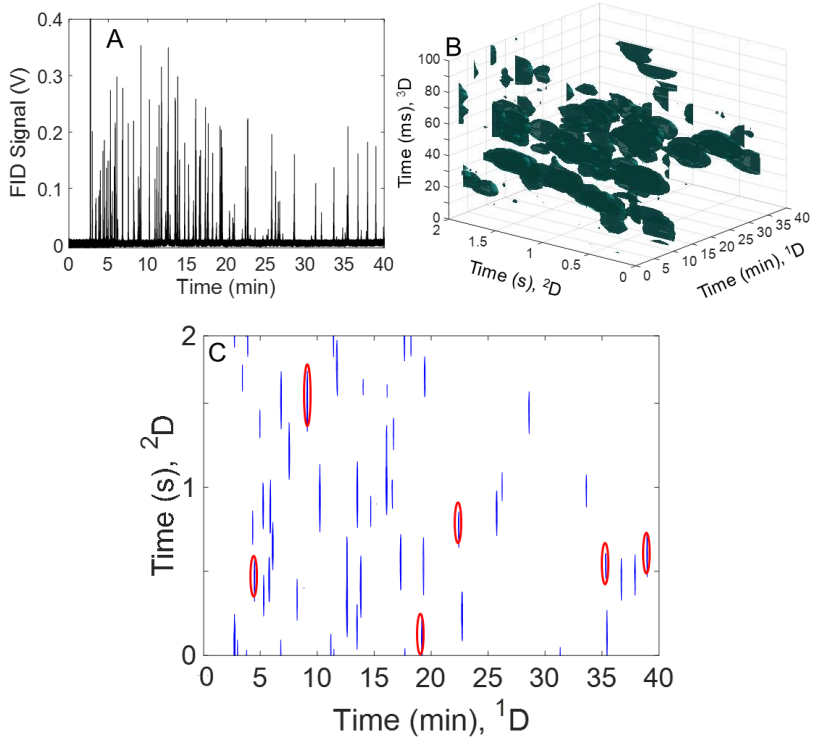

Figure 2.3 (A) Raw, preprocessed vector chromatogram for the GC^{3} separation of the 115-component mixture for the experiment. (B) Processed 3D isosurface plot of the entire separation. (C) Traditional, processed, ^{1}D × ^{2}D GC×GC chromatogram of the entire separation, where the data was summed along the ^{3}D axis. The six highlighted analytes, A-F, are further detailed in Table 2.2 for pertinent figures-of-merit. The volume of the data density in these macroscopic views detracts from quality of the chemical information contained in the separation. These views highlight the need for new ways to visualize and interpret complex samples and their data sets.

The 115-component test mixture was analyzed by GC^3 using the selected ${}^1\beta_r$ and ${}^2\beta_r$, with the columns indicated in the Experimental Section and summarized in Table 2.1. Fig. 2.3(A) displays the raw vector chromatogram prior to applying any data processing, which is not shown for brevity, but the steps are provided in previous reports [15,40]. Processing of the entire separation of analytes in Fig. 2.3(A), using the previously reported method [15], produces the isosurface "3D" plot in Fig. 2.3(B). The isosurface 3D plot in Fig. 2.3(B) highlights the potential for enhanced analytical information in GC^3 separations, but also the complexity of the plot emphasizes the challenges in how to effectively dissect and communicate the vast amount of information that is provided. Use of the GC^3 instrument necessitates new ways to visualize and interpret complex samples and the data sets produced. One way to simplify the viewing of the entire separation is presented in Fig. 2.3(C), which is the ${}^1D \times {}^2D$ chromatogram, where the separation data has been summed along the ${}^3D$ axis for the entire separation. Even in this "macroscopic" view, few details for the entire separation can be seen. The analyte peak widths on ${}^1D$, ${}^1W$, are extremely narrow when compared to the entire separation, with ${}^1W$ ranging from 4 to 6 s in a 2400 s (40 min) separation, and much of the detail regarding the sample and separation is not clear. Clarification of the exquisite 3D separation is provided by zooming in on short sections of the ${}^1D$ separation.

For close examination of a GC^3 separation, it becomes useful to "slice" the 3D data set into sections of time along the ${}^1D$ axis, as depicted in Fig. 2.1, for a given number of successive ${}^1D$ modulations. Each slice can span a user-selected segment of ${}^1D$ time (5-6 min, 33-38 min, etc.), and the researcher can elect to examine only the analytes that elute in this time span in a number of compact plots as presented in Figs 2.4(A-D). For example, Fig. 2.4(A) provides a zoom in view of the raw data in a 30 s window in the ${}^1D$ separation (approximately at the 20 min mark). The

partial modulation from the pulse flow valve is now seen on the modulations from the ^{2}D peaks to the ^{3}D separation, and a zoomed in view is provided in Fig. 2.4(B). Again, the raw data presented in Figs. 2.4(A-B) undergoes data processing [15] to become "apparent" peaks. Next, this data can be plotted in whole, as an isosurface 3D plot in Fig. 2.4(C), or the ^{1}D dimension can be summed away and a ^{2}D × ^{3}D chromatogram, such as Fig. 2.4(D), can be viewed.

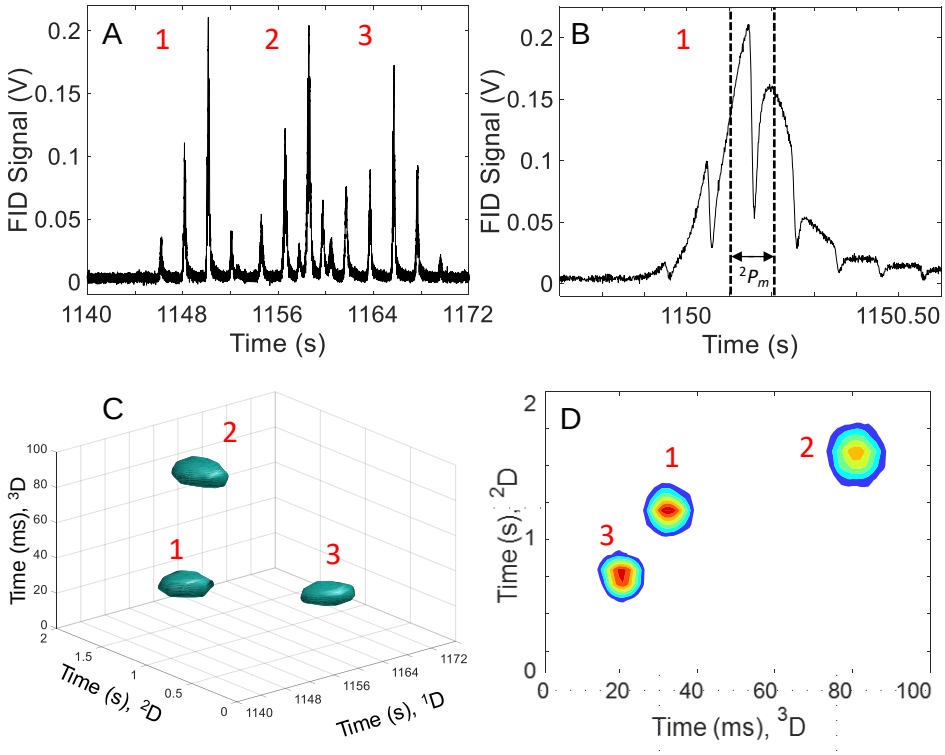

Figure 2.4 (A) Raw, preprocessed vector chromatogram for the GC^{3} separation at ~ 20 min (Analyte C in Fig. 2.3C). (B) Zoomed in view of the peak in Fig 2.4(A) with the highest signal intensity to show the pulse flow valve actuating on a ^{2}D peak. The pulse flow valve modulation period, $^{2}P_{M}$, is shown. (C) The three analytes from Fig. 2.4(A) processed and plotted in a 3D, isosurface plot. (D) A ^{2}D × ^{3}D GC×GC chromatogram, summed along the ^{1}D axis, for the same three analytes eluting as Fig. 2.4A. This "slice" of ^{1}D time, a 30 s window in this case, is more user-friendly to visualize and interpret and can be repeated for any time points of interest along a separation.

Comparing Figs. 2.4(C-D) to Figs. 2.3(B-C), one can quickly note the clarity of the information presented and the immediate utility of this less data-rich, "sliced" approach. By examining selected "slices" of the ^{1}D separation, the researcher can make useful determinations about the analytes that elute with less extraneous information. This process was performed in MatLab by cutting out segments of ^{1}D time (in data points) and then summing the data along the ^{1}D axis, thus leaving only ^{2}D and ^{3}D data to be plotted on a chromatogram based on the time that was "sliced." The GC^{3} instrument can more readily be used to identify analytes of interest within a complex sample by viewing the chromatograms as ^{2}D × ^{3}D at specific ^{1}D time points (determined by expected elution times based on analyte boiling points [14,15]).

2.4.2 *Peak Capacity Production*

Peak capacity and peak capacity production were both evaluated for this GC^{3} instrument for the two GC×GC column sets, ^{1}D × ^{2}D, and ^{2}D × ^{3}D [42]. Six representative analytes were selected spanning the range of retention times on all three dimensions for analysis of the ability of sustained peak capacity production by the GC^{3} instrument. The locations of these six representative analytes are highlighted in Fig. 2.3(C) and have their relevant peak width measurements (^{1}W, ^{2}W, and ^{3}W for ^{1}D, ^{2}D and ^{3}D, respectively) and figures-of-merit for peak capacity and peak capacity production provided in Table 2.2. Measurement of the peak widths and retention times on all three separation dimensions for each analyte is not shown for brevity, but was accomplished as presented previously [15]. There is an initial surge in peak capacity production within the first 10 min of the separation, and then the GC^{3} instrument appears to maintain a more consistent peak capacity production with minor variations in ^{1}W, ^{2}W, and ^{3}W from 10 to 40 min. The chosen temperature programming rate, along with the relatively lower $^{1}\beta$ of 112.5, produced relatively constant ^{1}W throughout the ^{1}D run. The minor changes in ^{2}W are

directly related to the ${}^{1}\beta_r$ of 0.45 and the control that this β_r provides over the T_e and thus the ${}^{2}k$ range that eluting analytes can exhibit. These six representative analytes average an ideal $n_{c,3D}$ of 30,600 over 40 min, or a sustained peak capacity production of 765 peaks/min. To calculate these amounts, Eq. (2.6) was used with the average ${}^{1}W$, ${}^{2}W$, and ${}^{3}W$ values in Table 2.2. Further work to reduce ${}^{1}W$ and ${}^{2}W$, or alternatively a drop in ${}^{1}\rho_s$ and ${}^{2}\rho_s$ values to ~2.0, according to Eqs. (2.6) and (2.8), can theoretically provide a peak capacity production well above 1,000 peaks/min, and an ideal 3D peak capacity $n_{c,3D}$ approaching 60,000 in a 40 min separation.

	Analyte A	Analyte B	Analyte C	Analyte D	Analyte E	Analyte F	Average
${}^{1}t_R$ (min)	4	10	20	22	35	40	--
${}^{1}W$ (s)	3	4	5.5	6	5	5	4.8
${}^{1}\rho_s$	1.5	2	2.8	3	2.5	2.5	2.4
${}^{2}W$ (ms)	266	356	358	342	341	359	337
${}^{2}\rho_s$	2.7	3.6	3.6	3.4	3.4	3.6	3.4
${}^{2}n_c$	7.5	5.6	5.6	5.8	5.8	5.5	6
${}^{3}W$ (ms)	8	10	10	10	10	10	9.7
${}^{3}n_c$	12.5	10	10	10	10	10	10.4
${}^{2}n_c * {}^{3}n_c$	93	56	56	58	58	55	62

Table 2.2 Chromatographic peak measurements and figures of merit for the 115-component mixture during the 40 min separation. See Fig. 2.3(C) for location of the analytes in the chromatograms. Using Eq. (2.6), the total nc,3D is calculated at 30,600 peaks, or a peak production capacity of 765 peaks/min for the 40 min separation.

Additionally, the complementary chemical selectivity provided by the semi-polar ^{2}D and polar ^{3}D are emphasized. Fig. 2.5(A) through (D) displays 2 of the 6 analytes listed in Table 2.2,

highlighting the selectivity differences in the $^{2}D \times {}^{3}D$ chromatograms relative to the $^{1}D \times {}^{2}D$ chromatograms at these time points along the ^{1}D separation. The exceptional separation efficiency in the ^{2}D and ^{3}D separations results in a high 2D peak capacity in the $^{2}D \times {}^{3}D$ plots, Fig. 2.5(B) and (D), which provide a 2D peak capacity of 93 and 56, respectively. Note that the chromatograms in Fig. 2.5(B) and (D) span a ^{1}D time of 14 and 32 s, respectively, but are done so to enable comparison of nearby analytes.

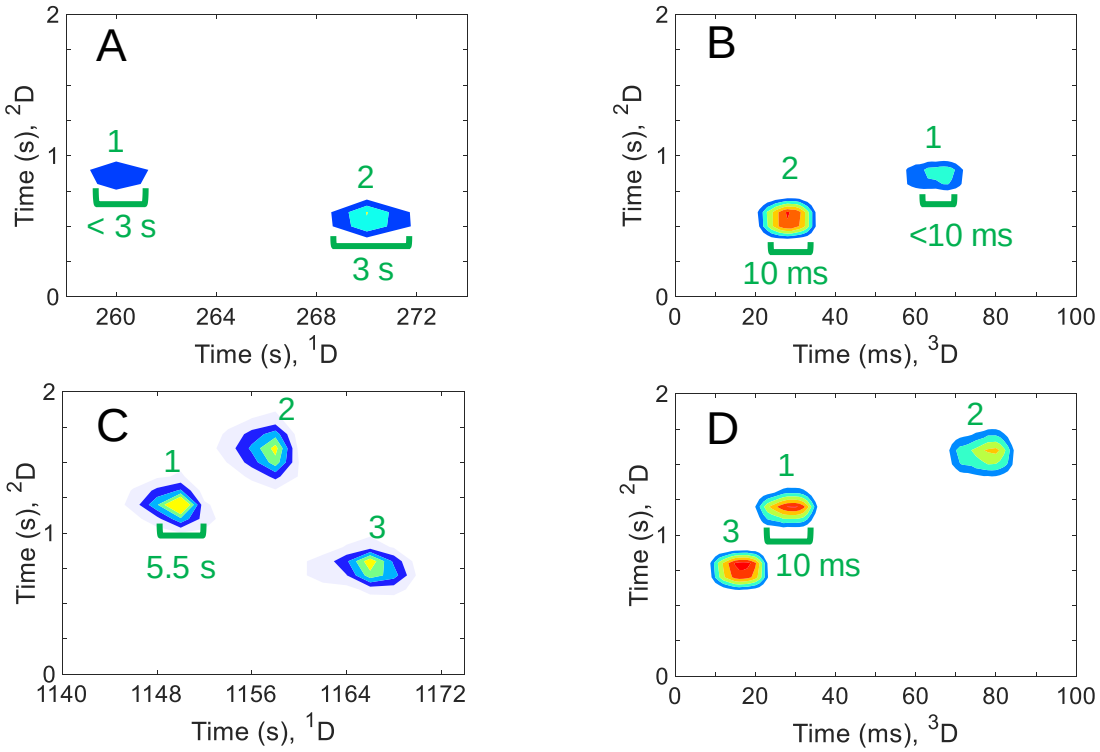

Figure 2.5 (A) Two sets of GC×GC chromatograms. The y-axis is held constant to show the ^{2}D for ease of comparison. Additionally, each analyte is numbered for comparison between (A) and (B), and (C) and (D). (A) Two analytes eluting at ~4 min on the ^{1}D axis. (B) The same two analytes from (A) on a $^{2}D \times {}^{3}D$ chromatogram, spanning the same ^{1}D axis time. Appropriate *W* measurements are shown to highlight the $n_{c,2D}$ of ~93 for the $^{2}D \times {}^{3}D$. (C) Three analytes eluting at ~20 min on the ^{1}D axis. (D) The same three analytes from (C) on a $^{2}D \times {}^{3}D$ chromatogram, spanning the same ^{1}D axis time. The *W* measurements are shown to highlight the $n_{c,2D}$ of ~56.

Peak capacity production is a useful figure-of-merit to compare the separation power of various GC-based instruments. Not only did we consider the total separation power of the GC^3 instrument, but we also realized its potential for further applications. As mentioned, looking at slices of time along the ^1D axis, snippets of time can be compared for a given $^2D \times {}^3D$ chromatogram. One can envisage the ^1D separation as providing a distillation process, with the $^2D \times {}^3D$ dimensions providing a GC×GC instrument with a 2D peak capacity approaching 100. These snapshots in time, which can be reduced to as low as the ^1P_M (2 s in this study), provides a near-real time snapshot of what is occurring on the ^1D column at any given point in time. In this case, the 2D peak capacity, averaging 55 peaks in this 2 s time window, holds great promise in observing chemical reactions in near real-time progression.

2.5 CONCLUSION

MDGC is an evolving field that continues to be challenged by increasingly complex samples. New hardware designs continue to be explored to solve emerging chemical analysis problems, and in particular, GC^3 appears to hold great promise, although it is still in its infancy stage of development. Various instrument parameters and hardware designs must be carefully chosen to maximize peak capacity and thus to appropriately separate, identify, and quantify analytes. However, the one hardware design variable often overlooked is the relation of successive phase volume ratios, β's, between separation dimensions and the resulting control one gets over analyte retention factors. This relation, termed the β ratio, β_r, is a key variable to control the relative k minimum and range available on the succeeding column for eluting analytes. Moreover, this control is provided throughout an entire ^1D run, whether it is a short 5-min separation or a long 40+ min separation. In this study, this control is displayed by the GC^3 instrument, with a peak capacity $n_{c,3D}$ of nearly 31,000 obtained in 40 min, with a peak capacity production averaging 765

peaks/min. The column selection strategy employed enabled this high, sustained peak capacity production over the course of the entire separation, as is particularly in evidence by Analytes D, E, and F in Table 2.2. The resulting peak capacity is nearly 4-fold higher than our previous report with GC^3 [15], and about 10-fold higher than typically obtained with GC×GC [15,22,35,38,40,41,52], which bodes well for the analysis of extremely complex samples.

2.6 REFERENCES

[1] Z. Liu, J.B. Phillips, Comprehensive two-dimensional gas chromatography using an on-column thermal modulator interface, J. Chromatogr. Sci. 29 (1991) 227–231. doi:10.1093/chromsci/29.6.227.

[2] H.D. Bean, J.-M.D. Dimandja, J.E. Hill, Bacterial volatile discovery using solid phase microextraction and comprehensive two-dimensional gas chromatography–time-of-flight mass spectrometry, J. Chromatogr. B. 901 (2012) 41–46. doi:10.1016/j.jchromb.2012.05.038.

[3] S. Prebihalo, A. Brockman, J. Cochran, F.L. Dorman, Determination of emerging contaminants in wastewater utilizing comprehensive two-dimensional gas-chromatography coupled with time-of-flight mass spectrometry, J. Chromatogr. A. 1419 (2015) 109–115. doi:10.1016/j.chroma.2015.09.080.

[4] P.-H. Stefanuto, K.A. Perrault, L.M. Dubois, B. L'Homme, C. Allen, C. Loughnane, N. Ochiai, J.-F. Focant, Advanced method optimization for volatile aroma profiling of beer using two-dimensional gas chromatography time-of-flight mass spectrometry, J. Chromatogr. A. 1507 (2017) 45–52. doi:10.1016/j.chroma.2017.05.064.

[5] L.M. Dubois, K.A. Perrault, P.-H. Stefanuto, S. Koschinski, M. Edwards, L. McGregor, J.-F. Focant, Thermal desorption comprehensive two-dimensional gas chromatography coupled to variable-energy electron ionization time-of-flight mass spectrometry for monitoring subtle changes in volatile organic compound profiles of human blood, J. Chromatogr. A. 1501 (2017) 117–127. doi:10.1016/j.chroma.2017.04.026.

[6] C.E. Freye, B.D. Fitz, M.C. Billingsley, R.E. Synovec, Partial least squares analysis of rocket propulsion fuel data using diaphragm valve-based comprehensive two-dimensional gas chromatography coupled with flame ionization detection, Talanta 153 (2016) 203–210. doi:10.1016/j.talanta.2016.03.016.

[7] P. Dimitriou-Christidis, A. Bonvin, S. Samanipour, J. Hollender, R. Rutler, J. Westphale, J. Gros, J.S. Arey, GC×GC Quantification of priority and emerging nonpolar halogenated micropollutants in all types of wastewater matrices: analysis methodology, chemical occurrence, and partitioning, Environ. Sci. Technol. 49 (2015) 7914–7925. doi:10.1021/es5049122.

[8] D. Megson, R. Kalin, P.J. Worsfold, C. Gauchotte-Lindsay, D.G. Patterson, M.C. Lohan, S. Comber, T.A. Brown, G. O'Sullivan, Fingerprinting polychlorinated biphenyls in environmental samples using comprehensive two-dimensional gas chromatography with time-of-flight mass spectrometry, J. Chromatogr. A. 1318 (2013) 276–283. doi:10.1016/j.chroma.2013.10.016.

[9] J.E. Welke, V. Manfroi, M. Zanus, M. Lazzarotto, C. Alcaraz Zini, Differentiation of wines according to grape variety using multivariate analysis of comprehensive two-dimensional gas chromatography with time-of-flight mass spectrometric detection data, Food Chem. 141 (2013) 3897–3905. doi:10.1016/j.foodchem.2013.06.100.

[10] D. Chen, J.H. Seo, J. Liu, K. Kurabayashi, X. Fan, Smart three-dimensional gas chromatography, Anal. Chem. 85 (2013) 6871–6875. doi:10.1021/ac401152v.

[11] N.E. Watson, W.C. Siegler, J.C. Hoggard, R.E. Synovec, Comprehensive three-dimensional gas chromatography with parallel factor analysis, Anal. Chem. 79 (2007) 8270–8280. doi:10.1021/ac070829x.

[12] W.C. Siegler, J.A. Crank, D.W. Armstrong, R.E. Synovec, Increasing selectivity in comprehensive three-dimensional gas chromatography via an ionic liquid stationary phase column in one dimension, J. Chromatogr. A. 1217 (2010) 3144–3149. doi:10.1016/j.chroma.2010.02.082.
[13] N.E. Watson, H.D. Bahaghighat, K. Cui, R.E. Synovec, Comprehensive three-dimensional gas chromatography with time-of-flight mass spectrometry, Anal. Chem. 89 (2017) 1793–1800. doi:10.1021/acs.analchem.6b04112.
[14] N.E. Watson, S.E. Prebihalo, R.E. Synovec, Targeted analyte deconvolution and identification by four-way parallel factor analysis using three-dimensional gas chromatography with mass spectrometry data, Anal. Chim. Acta (2017). doi:10.1016/j.aca.2017.06.017.
[15] H.D. Bahaghighat, C.E. Freye, D.V. Gough, P.E. Sudol, R.E. Synovec, Ultrafast separations via pulse flow valve modulation to enable high peak capacity multidimensional gas chromatography, J. Chromatogr. A. (2018). doi:10.1016/j.chroma.2018.08.001.
[16] M.S. Klee, J. Cochran, M. Merrick, L.M. Blumberg, Evaluation of conditions of comprehensive two-dimensional gas chromatography that yield a near-theoretical maximum in peak capacity gain, J. Chromatogr. A. 1383 (2015) 151–159. doi:10.1016/j.chroma.2015.01.031.
[17] J.M. Davis, Statistical theory of spot overlap for n-dimensional separations, Anal. Chem. 65 (1993) 2014–2023. doi:10.1021/ac00063a015.
[18] J.M. Davis, J.C. Giddings, Statistical theory of component overlap in multicomponent chromatograms, Anal. Chem. 55 (1983) 418–424. doi:10.1021/ac00254a003.
[19] J.M. Davis, J.C. Giddings, Statistical method for estimation of number of components from single complex chromatograms: theory, computer-based testing, and analysis of errors, Anal. Chem. 57 (1985) 2168–2177. doi:10.1021/ac00289a002.
[20] C.E. Freye, R.E. Synovec, High temperature diaphragm valve-based comprehensive two-dimensional gas chromatography with time-of-flight mass spectrometry, Talanta 161 (2016) 675–680. doi:10.1016/j.talanta.2016.09.002.
[21] A.M. Muscalu, M. Edwards, T. Górecki, E.J. Reiner, Evaluation of a single-stage consumable-free modulator for comprehensive two-dimensional gas chromatography: Analysis of polychlorinated biphenyls, organochlorine pesticides and chlorobenzenes, J. Chromatogr. A. 1391 (2015) 93–101. doi:10.1016/j.chroma.2015.02.074.
[22] J.V. Seeley, N.E. Schimmel, S.K. Seeley, The multi-mode modulator: A versatile fluidic device for two-dimensional gas chromatography, J. Chromatogr. A. 1536 (2018) 6–15. doi:10.1016/j.chroma.2017.06.030.
[23] J.B. Phillips, R.B. Gaines, J. Blomberg, F.W.M. van der Wielen, J.-M. Dimandja, V. Green, J. Granger, D. Patterson, L. Racovalis, H.-J. de Geus, J. de Boer, P. Haglund, J. Lipsky, V. Sinha, E.B. Ledford, A robust thermal modulator for comprehensive two-dimensional gas chromatography, J. High Resolut. Chromatogr. 22 (1999) 3–10. doi:10.1002/(SICI)1521-4168(19990101)22:1<3::AID-JHRC3>3.0.CO;2-U.
[24] J.B. Phillips, J. Xu, Comprehensive multi-dimensional gas chromatography, J. Chromatogr. A. 703 (1995) 327–334. doi:10.1016/0021-9673(95)00297-Z.
[25] P.J. Marriott, R.M. Kinghorn, Longitudinally modulated cryogenic system. A generally applicable approach to solute trapping and mobilization in gas chromatography, Anal. Chem. 69 (1997) 2582–2588. doi:10.1021/ac961310w.

[26] J. Harynuk, T. Górecki, Comprehensive two-dimensional gas chromatography in stop-flow mode, J. Sep. Sci. 27 (2004) 431–441. doi:10.1002/jssc.200301649.
[27] J.V. Seeley, N.J. Micyus, S.V. Bandurski, S.K. Seeley, J.D. McCurry, Microfluidic deans switch for comprehensive two-dimensional gas chromatography, Anal. Chem. 79 (2007) 1840–1847. doi:10.1021/ac061881g.
[28] P.A. Bueno, J.V. Seeley, Flow-switching device for comprehensive two-dimensional gas chromatography, J. Chromatogr. A. 1027 (2004) 3–10. doi:10.1016/j.chroma.2003.10.033.
[29] J.V. Seeley, Recent advances in flow-controlled multidimensional gas chromatography, J. Chromatogr. A. 1255 (2012) 24–37. doi:10.1016/j.chroma.2012.01.027.
[30] M. Edwards, A. Mostafa, T. Górecki, Modulation in comprehensive two-dimensional gas chromatography: 20 years of innovation, Anal. Bioanal. Chem. 401 (2011) 2335–2349. doi:10.1007/s00216-011-5100-6.
[31] J.F. Griffith, W.L. Winniford, K. Sun, R. Edam, J.C. Luong, A reversed-flow differential flow modulator for comprehensive two-dimensional gas chromatography, J. Chromatogr. A. 1226 (2012) 116–123. doi:10.1016/j.chroma.2011.11.036.
[32] H.-J. de Geus, J. de Boer, U.A.T. Brinkman, Development of a thermal desorption modulator for gas chromatography, J. Chromatogr. A. 767 (1997) 137–151. doi:10.1016/S0021-9673(97)00038-1.
[33] J.B. Phillips, E.B. Ledford, Thermal modulation: A chemical instrumentation component of potential value in improving portability, Field Anal. Chem. Technol. 1 (1996) 23–29. doi:10.1002/(SICI)1520-6521(1996)1:1<23::AID-FACT4>3.0.CO;2-F.
[34] H.-J. de Geus, A. Schelvis, J. de Boer, U.A.Th. Brinkman, Comprehensive two-dimensional gas chromatography with a rotating thermal desorption modulator and independently temperature-programmable columns, J. High Res. Chromatogr. 23 (2000) 189–196. doi:10.1002/(SICI)1521-4168(20000301)23:3<189::AID-JHRC189>3.0.CO;2-N.
[35] E.B. Ledford, C. Billesbach, Jet-cooled thermal modulator for comprehensive multidimensional gas chromatography, J. High Res. Chromatogr. 23 (2000) 202–204. doi:10.1002/(SICI)1521-4168(20000301)23:3<202::AID-JHRC202>3.0.CO;2-5.
[36] J. Beens, M. Adahchour, R.J.J. Vreuls, K. van Altena, U.A. Th. Brinkman, Simple, non-moving modulation interface for comprehensive two-dimensional gas chromatography, J. Chromatogr. A. 919 (2001) 127–132. doi:10.1016/S0021-9673(01)00785-3.
[37] J.V. Seeley, F. Kramp, C.J. Hicks, Comprehensive two-dimensional gas chromatography via differential flow modulation, Anal. Chem. 72 (2000) 4346–4352. doi:10.1021/ac000249z.
[38] C. Duhamel, P. Cardinael, V. Peulon-Agasse, R. Firor, L. Pascaud, G. Semard-Jousset, P. Giusti, V. Livadaris, Comparison of cryogenic and differential flow (forward and reverse fill/flush) modulators and applications to the analysis of heavy petroleum cuts by high-temperature comprehensive gas chromatography, J. Chromatogr. A. 1387 (2015) 95–103. doi:10.1016/j.chroma.2015.01.095.
[39] H. Cai, S.D. Stearns, Partial modulation method via pulsed flow modulator for comprehensive two-dimensional gas chromatography, Anal. Chem. 76 (2004) 6064–6076. doi:10.1021/ac0492463.
[40] C.E. Freye, H.D. Bahaghighat, R.E. Synovec, Comprehensive two-dimensional gas chromatography using partial modulation via a pulsed flow valve with a short modulation period, Talanta 177 (2018) 142–149. doi:10.1016/j.talanta.2017.08.095.

[41] H.D. Bahaghighat, C.E. Freye, R.E. Synovec, Recent advances in modulator technology for comprehensive two dimensional gas chromatography, TrAC Trends Anal. Chem. (2018). doi:10.1016/j.trac.2018.04.016.
[42] B.A. Parsons, D.K. Pinkerton, R.E. Synovec, Implications of phase ratio for maximizing peak capacity in comprehensive two-dimensional gas chromatography time-of-flight mass spectrometry, J. Chromatogr. A. 1536 (2018) 16–26. doi:10.1016/j.chroma.2017.07.018.
[43] L. Mahé, M. Courtiade, C. Dartiguelongue, J. Ponthus, V. Souchon, D. Thiébaut, Overcoming the high-temperature two-dimensional gas chromatography limits to elute heavy compounds, J. Chromatogr. A. 1229 (2012) 298–301. doi:10.1016/j.chroma.2012.01.030.
[44] M.S. Klee, GC inlets an introduction, second, Agilent Technogies, Inc., Wilmington, DE USA, 2005. http://www.agilent.com/cs/library/usermanuals/public/5958-9468_041007.pdf.
[45] L.M. Blumberg, Flow optimization in one-dimensional and comprehensive two-dimensional gas chromatography, J. Chromatogr. A. 1536 (2018) 27–38. doi:10.1016/j.chroma.2017.08.040.
[46] L.M. Blumberg, Linear peak capacity of a comprehensive multi-dimensional separation, J. Sep. Sci. 31 (2008) 3352–3357. doi:10.1002/jssc.200800244.
[47] D.R. Stoll, X. Wang, P.W. Carr, Comparison of the practical resolving power of one- and two-dimensional high-performance liquid chromatography analysis of metabolomic samples, Anal. Chem. 80 (2008) 268–278. doi:10.1021/ac701676b.
[48] J.C. Giddings, Unified separation science, Wiley, New York, 1991. http://catalog.hathitrust.org/api/volumes/oclc/21764363.html (accessed June 8, 2016).
[49] L.M. Blumberg, Accumulating resampling (modulation) in comprehensive two-dimensional capillary GC (GC×GC), J. Sep. Sci. 31 (2008) 3358–3365. doi:10.1002/jssc.200800424.
[50] W. Khummueng, J. Harynuk, P.J. Marriott, Modulation ratio in comprehensive two-dimensional gas chromatography, Anal. Chem. 78 (2006) 4578–4587. doi:10.1021/ac052270b.
[51] W.C. Siegler, B.D. Fitz, J.C. Hoggard, R.E. Synovec, Experimental study of the quantitative precision for valve-based comprehensive two-dimensional gas chromatography, Anal. Chem. 83 (2011) 5190–5196. doi:10.1021/ac200302b.
[52] A.C. Beckstrom, E.M. Humston, L.R. Snyder, R.E. Synovec, S.E. Juul, Application of comprehensive two-dimensional gas chromatography with time-of-flight mass spectrometry method to identify potential biomarkers of perinatal asphyxia in a non-human primate model, J. Chromatogr. A 1218 (2011) 1899–1906. doi:10.1016/j.chroma.2011.01.086.

Chapter 3. Development of Partial Modulation: The Negative Pulse Mode for Gas Chromatographic Separations

3.1 INTRODUCTION

Comprehensive two-dimensional (2D) gas chromatography (GC×GC) has rapidly evolved since its first description by Giddings[1] and implementation by Liu and Phillips in 1991 [2]. The addition of the modulator enables eluate to be trapped after exiting the first separation column, focused, and re-injected on a second capillary column for second, faster separation. The modulator will perform this trapping and re-injecting at a set frequency, termed the modulation period (P_M). This transforms the relatively wide first dimension (^{1}D) peak into a series of sharper, taller second dimension (^{2}D) peaks that follow the same general shape as the ^{1}D peak. This ^{2}D enables up to a 10- to 20- fold increase in total peak capacity ($n_{c,2D}$) over traditional one-dimensional GC (1D-GC) [3–7].

The heart of all GC×GC instruments is the modulator. Multiple designs have been proposed and implemented since the original report, and they fall broadly into two categories: thermal and flow-based modulators [8,9]. Thermal modulators, as the name implies, use a cold area to trap analytes and then periodically reheats the trapped area to desorb the trapped analytes for subsequent separation [10–12]. Thermal modulators have the benefit of transferring all the eluate (duty cycle = 1.0) from the ^{1}D to the ^{2}D column. Flow-based modulators originated from heart-cutting GC-GC, where a Deans switch was used to transfer a portion of the eluate from the 1D column to a 2D column [13]. The Deans switch was adapted to become a flow modulator, able to focus a portion of the eluate (duty cycle < 1.0) from the 1D to the 2D column [14]. While there is generally a loss of analyte from the 1D to the 2D this has been shown to still be comprehensive [15], i.e. every analyte is still modulated and is seen by the detector despite some loss. Flow

modulators are generally seen as providing simplicity, lower operational costs, and can operate over a wider volatility range than thermal modulators [16–19].

Nearly all current modulators rely upon what has been termed "full modulation" methods. Modulators trap the entirety of the analyte signal eluting from the ^{1}D column and transfers it to the ^{2}D column, with analysts able to mathematically fit a gaussian function to the maxima of the ^{2}D peaks to regain ^{1}D figures of merit (such as retention time, $^{1}t_{r}$, and width-at-base, $^{1}w_{b}$) [20,21]. However, this additional analysis step was addressed by pioneering work into what is termed "partial modulation" by Cai and Stearns [22]. As the name implies, only a portion of the analyte is modulated, superimposing the ^{2}D separation on the ^{1}D profile. As originally illustrated with simulated data, partial modulation provides the possibility of mathematically retaining and isolating the 1D and 2D profiles [22]. Despite the unique and beneficial attributes of partial modulation, this form of modulation remains in its infancy in development.

Inspired by the original report, we have used a commercially available pulse flow valve to study the effects of partial modulation in the "positive pulse" mode, where a small pulse of carrier gas is injected at a T-union between the ^{1}D and ^{2}D columns [23–26]. Each pulse created a local vacancy in the analyte concentration profile, and as originally hypothesized, this vacancy contains the chemical information of the ^{2}D separation. Combining the principles of vacancy chromatography with frontal analysis chromatography, one can differentiate and invert the vacancies to produce "apparent" peaks [23]. These "apparent" peaks contain all the necessary chemical information for the analyst in 1D-GC, GC×GC, and comprehensive three-dimensional GC (GC^{3}), are reproducible, and can be used for quantification and chemometric analysis [23–26]. Additionally, the positive pulse mode generated narrow peak widths-at-base, w_{b} (4σ), as low

as single-digit ms, enabling high peak capacities for GC×GC (~11,000 in 11 min)[24] and GC3 (~31,000 in 40 min) [26] instruments.

Despite the beneficial attributes of this modulator operating in the positive pulse mode, the need to differentiate the signal (additional chemometric step) resulted in a loss of signal-to-noise ratio (*S/N*), making it generally unappealing for wide acceptance. Upon further study of the original report, it was realized that we had only attempted one of the forms of partial modulation, the positive pulse mode. There remains another unstudied form of partial modulation, which has been termed the negative pulse mode.

3.1.1 *Negative Pulse Mode, Partial Modulation Theory*

In the positive pulse mode, the pulsed flow valve modulator modulates the analytes as they exit the ^{1}D column by injecting a narrow pulse of carrier gas perpendicular to the flow at the T-union that joins the ^{1}D and ^{2}D separation columns. Here, we control how long the pulse flow valve is open and by how much we dilute (inject a vacancy into) the analyte stream. Conversely, we can control how long the pulse flow valve is *closed*, and thus we control how much of the analyte stream becomes *undiluted* at the T-union, as illustrated in Fig 3.1. During normal operation (Fig. 3.1A), the pulse flow valve is open, allowing an auxiliary flow of carrier gas to dilute the analyte stream at the T-union. During modulation (Fig. 3.1B), the pulse flow valve closes, allowing a small segment of the ^{1}D analyte stream to enter the ^{2}D column undiluted. When the pulse flow valve opens again (Fig. 3.1C), the analyte stream returns to its diluted state and the undiluted section will be the only section to undergo visible separation on the ^{2}D column. Visually, this expresses itself as the ^{2}D peaks superimposed ontop of the ^{1}D analyte profile (Fig 3.1D).

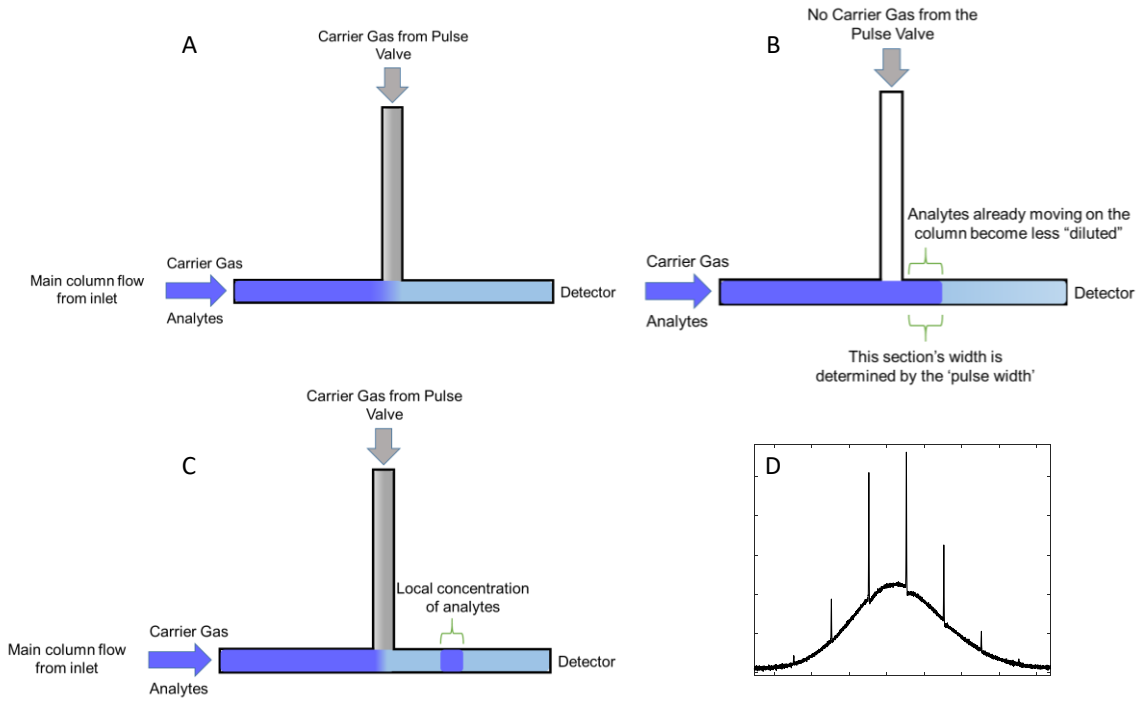

Figure 3.1 (A) In normal operation, the pulse flow valve is left open, allowing an auxiliary flow of carrier gas to dilute the analyte stream. (B) During modulation, the pulse valve closes, allowing an undiluted analyte segment from the 1D to enter the 2D. (C) The pulse valve opens, returning the flow of analytes back to its diluted state. (D) An example of the resulting raw data for the negative pulse mode.

These two extremes for partial modulation can be related to each other by their pulse widths (p_w). In the positive pulse mode, the pulse width ($p_{w,ppm}$) is how long the pulse flow valve is open. In the negative pulse mode, the pulse width ($p_{w,npm}$) is how long the pulse flow valve is closed. When combined, we find Equation 1

$$p_{w,ppm} + p_{w,ppm} = P_M \quad (1)$$

When $p_{w,ppm} << p_{w,npm}$, we are in the positive pulse mode and obtain negative peaks. When $p_{w,ppm} >> p_{w,npm}$, we are in the negative pulse mode and obtain positive peaks.

3.2 EXPERIMENTAL

This initial study was carried out on an Agilent 7890A GC and a 7683B auto injector (Agilent Technologies, Palo Alto, CA, USA). The stock electrometer for the Agilent FID was replaced with a built-in-house, high-speed electrometer which can collect data at 100 kHz. The electrometer was interfaced to a data acquisition board and data collection was collected using an in-house written LabVIEW program (National Instruments, Austin, TX, USA). Post-run data processing was performed in MATLAB R2017b (The Mathworks, Inc., Natick, MA, USA). All studies used an inlet temperature of 175 °C and an FID temperature of 255 °C.

The pulse flow valve (Model 009-0347-900, Parker Hannifin, Hollis, NH, USA) was mounted outside the oven with a custom-built fitting to connect a 125 µm inner diameter (ID) stainless steel tubing (VICI model T5C5D, Valco Instruments Company Inc., Houston, TX, USA) to a 3-way T-union (Model MT.5CXS6, Valco Instruments Company Inc., Houston, TX, USA). The pulse flow valve was controlled with an Iota One Microfluidic Valve Driver (Model 060-0010-900, Parker Hannifin, Hollis, NH, USA). All pressures and flow rates were controlled by the stock gauges in the GC platform.

The GC instrument was configured for a 1D-GC (Fig 3.2) mode. In this configuration, 50 µL of analytes was injected via a guard column (Restek, 25 cm × 100 µm ID) to a headspace sampling vial (Part Number 8010-0412, Agilent Technologies, Palo Alto, CA, USA), and a pseudo steady-state stream of analytes was delivered to the T-union via a second guard column (Restek, 25 cm × 100 µm ID). The separation column (DB-5, 1.0 m × 100 µm d_c × 0.10 µm d_f). The

separation was kept isothermal, with constant flow rates and pressure rates applied based on the experiment.

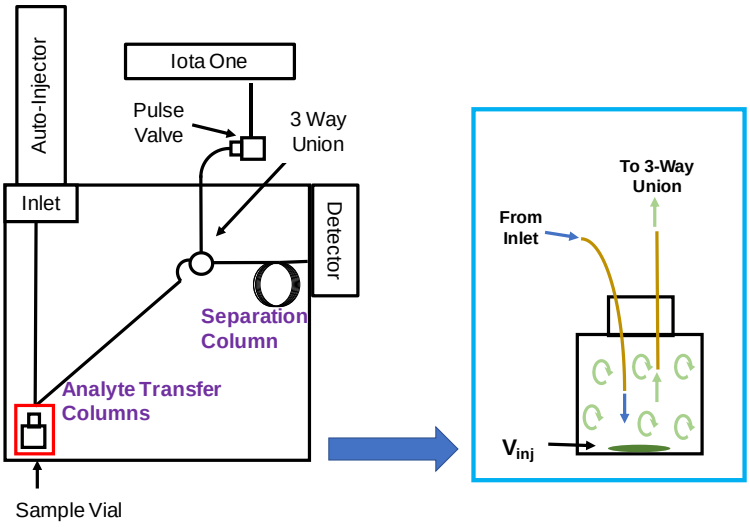

Figure 3.2 The GC instrument installed with a pulse flow valve modulator, in the headspace sampling mode (1D-GC). A zoom-in of the highlighted region is provided.

3.3 Results and Discussion

We begin by studying the negative pulse mode in a 1D-GC mode. By applying a pseudo steady-state analyte mixture to the modulator, the pulse flow valve becomes an injector onto a short, 1.0 m 1D-GC separation. Additionally, the high sampling (injecting) frequency capable by the pulse flow valve enables a rapid means to obtain replicate chromatograms to ensure reproducibility of the modulation technique. The first study used the alkanes C6-C10 (Fig 3.3) to determine the separation potential of this modulation technique. The oven was set to an isothermal temperature of 125 °C. The pressure of the auxiliary flow at the pulse flow valve

(23.0 psig) was closely matched to the pressure at the inlet (23.7 psig), and a $p_{w,npm}$ of 8 ms was applied. A relatively stable, elevated baseline is seen (Fig 3.3A) from the stream of analytes that

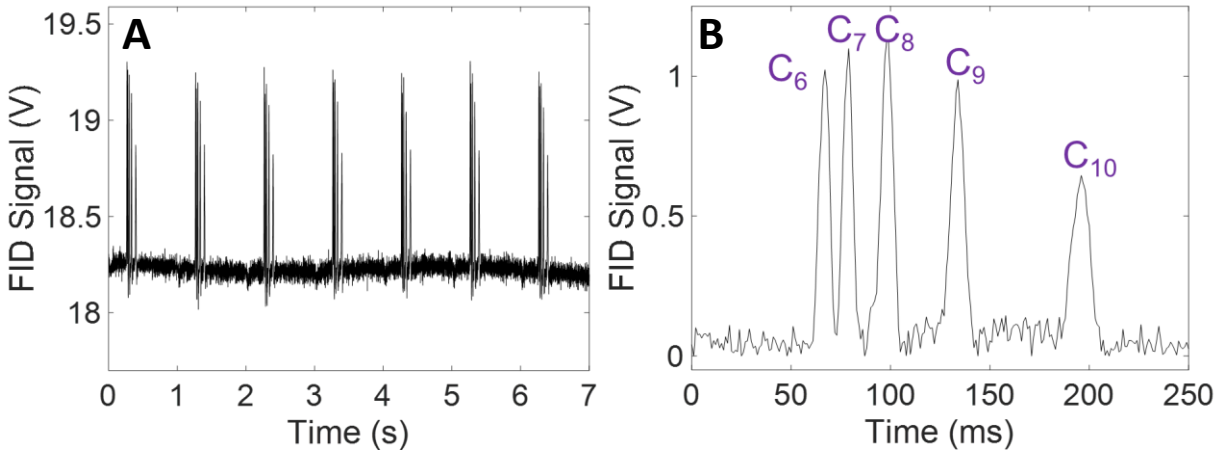

Figure 3.3 (A) The raw data of 7 successive injections of C6-C10 in the 1D-GC configuration. (B) Zoom-in view of the first injection (modulation) after baseline correction.

is constantly evaporating and entering the T-union. After a dead time (t_0) of approximately 60 ms, all 5 alkanes elute within 130 ms, with baseline resolution between each analyte (Fig. 3.3B). These 5 alkanes can elute this well separated due to the narrow w_b produced by the modulation method, with w_b ranging from 9.3 ms (C_6) to 10.1 ms (C_8) to 14.8 ms (C_{10}).

Next, a more complicated separation was tested on the 1D-GC configuration. Using an isothermal temperature of 100 °C, 12 analytes were injected (~50 µL) into the headspace vial for subsequent separation. The pressure of the auxiliary flow at the pulse flow valve (48.5 psig) was closely matched to the pressure at the inlet (47.6 psig), and a $p_{w,npm}$ of 10 ms was applied with. After baseline correction, we found a similar, powerful separation (Fig. 3.4). After a t_0 of approximately 90 ms, the 12 analytes again elute with baseline resolution between them (Fig. 3.4). The order of elution is: acetone, heptane, octane, chlorobenzene, nonane, butylbenzene, decane,

benzyl alcohol, undecane, 1-octanethiol, nonanol, and dodecane. The separating power of this modulation method is apparent, as there is baseline resolution between all peaks, with all 12 eluting within 500 ms of each other (Fig 3.4B).

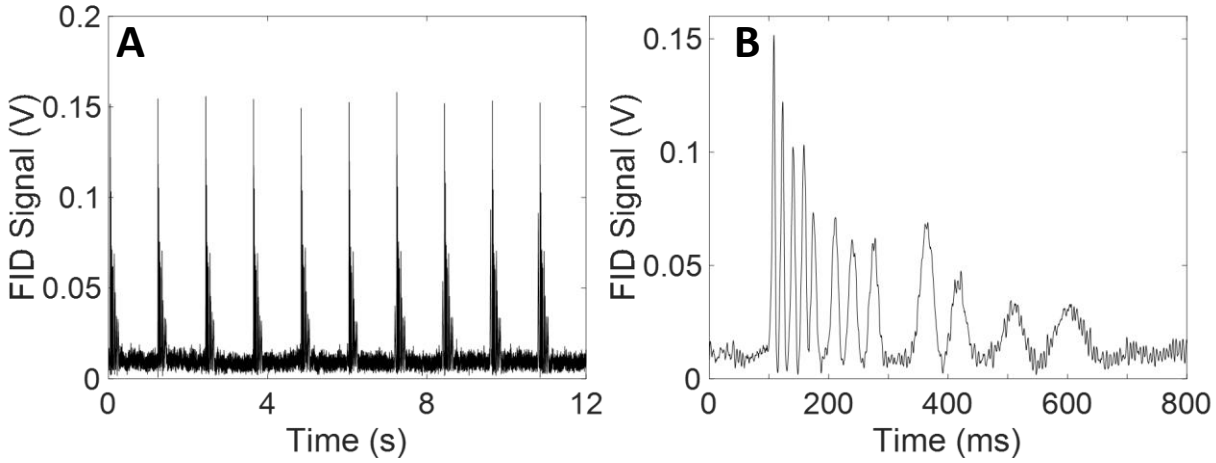

Figure 3.4 (A) The raw data of 10 successive injections of the 12 mix in the 1D-GC configuration. (B) Zoom-in view of the first injection (modulation) after baseline correction. The order of elution is: acetone, heptane, octane, chlorobenzene, nonane, butylbenzene, decane, benzyl alcohol, undecane, 1-octanethiol, nonanol, and dodecane.

Additionally, this 1D-GC study presents an intriguing way to imagine the use of any GC instrument. In this 1D-GC mode, the pulse valve is attached to a regular GC instrument. One can imagine, instead of a headspace vial, that a process or chemical reaction that emits volatile compounds can be monitored by supplying the T-union with a steady stream of analytes. This enables the already powerful (and at times expensive) instruments that are currently present in industrial facilities can be easily modified to provide continuous monitoring, or even on-line analysis, of chemical processes.

3.4 CONCLUSION

In this work, further development of the concept of partial modulation in the negative pulse mode is presented. The negative pulse mode has proven to be a powerful separation technique that enables the production of very narrow w_b after modulation. The ability to separate this series of light, volatile organic compounds on such short time frames (< 500 ms) with baseline resolution between each analyte is a remarkable development for high-speed GC. Additional investigations on the relationship between w_b of the pulse flow valve to signal intensity and w_b of the analyte are warranted. Moreover, using this modulation technique as the second dimension of a GC×GC instrument will yield remarkably high peak capacities in short P_M, as evidenced by the 1D-GC studies.

3.5 REFERENCES

[1] J.C. Giddings, Unified separation science, Wiley, New York, 1991. http://catalog.hathitrust.org/api/volumes/oclc/21764363.html.

[2] Z. Liu, J.B. Phillips, Comprehensive two-dimensional gas chromatography using an on-column thermal modulator interface, J. Chromatogr. Sci. 29 (1991) 227–231. doi:10.1093/chromsci/29.6.227.

[3] J.M. Davis, Statistical theory of spot overlap for n-dimensional separations, Anal. Chem. 65 (1993) 2014–2023. doi:10.1021/ac00063a015.

[4] L.M. Blumberg, F. David, M.S. Klee, P. Sandra, Comparison of one-dimensional and comprehensive two-dimensional separations by gas chromatography, J. Chromatogr A. 1188 (2008) 2–16. doi:10.1016/j.chroma.2008.02.044.

[5] M.S. Klee, J. Cochran, M. Merrick, L.M. Blumberg, Evaluation of conditions of comprehensive two-dimensional gas chromatography that yield a near-theoretical maximum in peak capacity gain, J. Chromatogr A. 1383 (2015) 151–159. doi:10.1016/j.chroma.2015.01.031.

[6] J.M. Davis, J.Calvin. Giddings, Statistical theory of component overlap in multicomponent chromatograms, Anal. Chem. 55 (1983) 418–424. doi:10.1021/ac00254a003.

[7] J.M. Davis, J.Calvin. Giddings, Statistical method for estimation of number of components from single complex chromatograms: theory, computer-based testing, and analysis of errors, Anal. Chem. 57 (1985) 2168–2177. doi:10.1021/ac00289a002.

[8] S.E. Prebihalo, K.L. Berrier, C.E. Freye, H.D. Bahaghighat, N.R. Moore, D.K. Pinkerton, R.E. Synovec, Multidimensional gas chromatography: advances in instrumentation, chemometrics, and applications, Anal. Chem. (2017). doi:10.1021/acs.analchem.7b04226.

[9] H.D. Bahaghighat, C.E. Freye, R.E. Synovec, Recent advances in modulator technology for comprehensive two dimensional gas chromatography, TrAC Trends Anal. Chem. (2018). doi:10.1016/j.trac.2018.04.016.

[10] P.J. Marriott, R.M. Kinghorn, Longitudinally modulated cryogenic system. A generally applicable approach to solute trapping and mobilization in gas chromatography, Anal. Chem. 69 (1997) 2582–2588. doi:10.1021/ac961310w.

[11] E.B. Ledford, C. Billesbach, Jet-cooled thermal modulator for comprehensive multidimensional gas chromatography, J. High Resolut. Chromatogr. 23 (2000) 202–204. doi:10.1002/(SICI)1521-4168(20000301)23:3<202::AID-JHRC202>3.0.CO;2-5.

[12] J. Beens, M. Adahchour, R.J.J. Vreuls, K. van Altena, U.A. Th. Brinkman, Simple, non-moving modulation interface for comprehensive two-dimensional gas chromatography, J. Chromatogr A. 919 (2001) 127–132. doi:10.1016/S0021-9673(01)00785-3.

[13] D.R. Deans, A new technique for heart cutting in gas chromatography [1], Chromatographia. 1 (1968) 18–22. doi:10.1007/BF02259005.

[14] J.V. Seeley, F. Kramp, C.J. Hicks, Comprehensive two-dimensional gas chromatography via differential flow modulation, Anal. Chem. 72 (2000) 4346–4352. doi:10.1021/ac000249z.

[15] J.V. Seeley, Theoretical study of incomplete sampling of the first dimension in comprehensive two-dimensional chromatography, J. Chromatogr A. 962 (2002) 21–27. doi:10.1016/S0021-9673(02)00461-2.

[16] J.V. Seeley, N.J. Micyus, S.V. Bandurski, S.K. Seeley, J.D. McCurry, Microfluidic deans switch for comprehensive two-dimensional gas chromatography, Anal. Chem. 79 (2007) 1840–1847. doi:10.1021/ac061881g.
[17] J.V. Seeley, Recent advances in flow-controlled multidimensional gas chromatography, J. Chromatogr A. 1255 (2012) 24–37. doi:10.1016/j.chroma.2012.01.027.
[18] M. Edwards, A. Mostafa, T. Górecki, Modulation in comprehensive two-dimensional gas chromatography: 20 years of innovation, Anal. Bioanal. Chem. 401 (2011) 2335–2349. doi:10.1007/s00216-011-5100-6.
[19] C. Duhamel, P. Cardinael, V. Peulon-Agasse, R. Firor, L. Pascaud, G. Semard-Jousset, P. Giusti, V. Livadaris, Comparison of cryogenic and differential flow (forward and reverse fill/flush) modulators and applications to the analysis of heavy petroleum cuts by high-temperature comprehensive gas chromatography, J. Chromatogr A. 1387 (2015) 95–103. doi:10.1016/j.chroma.2015.01.095.
[20] W. Khummueng, J. Harynuk, P.J. Marriott, Modulation ratio in comprehensive two-dimensional gas chromatography, Anal. Chem. 78 (2006) 4578–4587. doi:10.1021/ac052270b.
[21] W.C. Siegler, B.D. Fitz, J.C. Hoggard, R.E. Synovec, Experimental study of the quantitative precision for valve-based comprehensive two-dimensional gas chromatography, Anal. Chem. 83 (2011) 5190–5196. doi:10.1021/ac200302b.
[22] H. Cai, S.D. Stearns, Partial modulation method via pulsed flow modulator for comprehensive two-dimensional gas chromatography, Anal. Chem. 76 (2004) 6064–6076. doi:10.1021/ac0492463.
[23] C.E. Freye, H.D. Bahaghighat, R.E. Synovec, Comprehensive two-dimensional gas chromatography using partial modulation via a pulsed flow valve with a short modulation period, Talanta 177 (2018) 142–149. doi:10.1016/j.talanta.2017.08.095.
[24] H.D. Bahaghighat, C.E. Freye, D.V. Gough, P.E. Sudol, R.E. Synovec, Ultrafast separations via pulse flow valve modulation to enable high peak capacity multidimensional gas chromatography, J. Chromatogr A. 1573 (2018) 115–124. doi:10.1016/j.chroma.2018.08.001.
[25] H.D. Bahaghighat, C.E. Freye, D.V. Gough, R.E. Synovec, Comprehensive two-dimensional gas chromatography and time-of-flight mass spectrometry detection with a 50 ms modulation period, J. Chromatogr A. (2018). doi:10.1016/j.chroma.2018.11.027.
[26] D.V. Gough, H.D. Bahaghighat, R.E. Synovec, Column selection approach to achieve a high peak capacity in comprehensive three-dimensional gas chromatography, Talanta 195 (2019) 822–829. doi:10.1016/j.talanta.2018.12.007.

Chapter 4. Conclusion

Analytical chemists continue to investigate and develop new techniques and technologies to analyze ever-increasingly complex samples. After nearly 30 years of research and innovation in the field of multidimensional gas chromatography, continued improvements to the physical separation space of analytes is needed to handle these more challenging samples. Our work to this point has helped to address this need for increase physical separation space for analytes (Chapter 2). The availability of the pulse flow valve modulator, which can modulate as quickly as every 100 ms, provides the ability to add a fully optimized ^{3}D to a GC×GC instrument, providing the physical separation space to isolate up to 1,000 peaks/min (peak capacity production). This amount of physical separation space is currently unparalleled. Additionally, the pulse flow valve, operating as a partial modulator, provides incredible resolution between volatile organic compounds in short separations (Chapter 3). Continued research into the ultrafast potential of this modulator, operating in a 1D-GC as an injector, can lead to the GC being more useful to industries in need of powerful continuous monitoring technologies. Even mature analytical techniques, such as gas chromatography, can see bright new growth and evolution to increase their utility, applicability, and power.

BIBLIOGRAPHY

H.D. Bahaghighat, C.E. Freye, R.E. Synovec, Recent advances in modulator technology for comprehensive two-dimensional gas chromatography, TrAC, Trends Anal. Chem. (2018). doi:10.1016/j.trac.2018.04.016.

H.D. Bahaghighat, C.E. Freye, D.V. Gough, P.E. Sudol, R.E. Synovec, Ultrafast separations via pulse flow valve modulation to enable high peak capacity multidimensional gas chromatography, J. Chromatogr A. 1573 (2018) 115–124. doi:10.1016/j.chroma.2018.08.001.

H.D. Bahaghighat, C.E. Freye, D.V. Gough, R.E. Synovec, Comprehensive two-dimensional gas chromatography and time-of-flight mass spectrometry detection with a 50 ms modulation period, J. Chromatogr A. (2018). doi:10.1016/j.chroma.2018.11.027.

H.D. Bean, J.-M.D. Dimandja, J.E. Hill, Bacterial volatile discovery using solid phase microextraction and comprehensive two-dimensional gas chromatography–time-of-flight mass spectrometry, J. Chromatogr. B. 901 (2012) 41–46. doi:10.1016/j.jchromb.2012.05.038.

A.C. Beckstrom, E.M. Humston, L.R. Snyder, R.E. Synovec, S.E. Juul, Application of comprehensive two-dimensional gas chromatography with time-of-flight mass spectrometry method to identify potential biomarkers of perinatal asphyxia in a non-human primate model, J. Chromatogr. A. 1218 (2011) 1899–1906. doi:10.1016/j.chroma.2011.01.086.

J. Beens, M. Adahchour, R.J.J. Vreuls, K. van Altena, U.A. Th. Brinkman, Simple, non-moving modulation interface for comprehensive two-dimensional gas chromatography, J. Chromatogr A. 919 (2001) 127–132. doi:10.1016/S0021-9673(01)00785-3.

P.A. Bueno, J.V. Seeley, Flow-switching device for comprehensive two-dimensional gas chromatography, J. Chromatogr. A. 1027 (2004) 3–10. doi:10.1016/j.chroma.2003.10.033.

L.M. Blumberg, Accumulating resampling (modulation) in comprehensive two-dimensional capillary GC (GC×GC), J. Sep. Sci. 31 (2008) 3358–3365. doi:10.1002/jssc.200800424.

L.M. Blumberg, F. David, M.S. Klee, P. Sandra, Comparison of one-dimensional and comprehensive two-dimensional separations by gas chromatography, J. Chromatogr A. 1188 (2008) 2–16. doi:10.1016/j.chroma.2008.02.044.

L.M. Blumberg, Linear peak capacity of a comprehensive multi-dimensional separation, J. Sep. Sci. 31 (2008) 3352–3357. doi:10.1002/jssc.200800244.

L.M. Blumberg, Flow optimization in one-dimensional and comprehensive two-dimensional gas chromatography, J. Chromatogr. A. 1536 (2018) 27–38. doi:10.1016/j.chroma.2017.08.040.

H. Cai, S.D. Stearns, Partial modulation method via pulsed flow modulator for comprehensive two-dimensional gas chromatography, Anal. Chem. 76 (2004) 6064–6076. doi:10.1021/ac0492463.

D. Chen, J.H. Seo, J. Liu, K. Kurabayashi, X. Fan, Smart three-dimensional gas chromatography, Anal. Chem. 85 (2013) 6871–6875. doi:10.1021/ac401152v.

J.M. Davis, J. Calvin. Giddings, Statistical theory of component overlap in multicomponent chromatograms, Anal. Chem. 55 (1983) 418–424. doi:10.1021/ac00254a003.

J.M. Davis, J. Calvin. Giddings, Statistical method for estimation of number of components from single complex chromatograms: theory, computer-based testing, and analysis of errors, Anal. Chem. 57 (1985) 2168–2177. doi:10.1021/ac00289a002.

J.M. Davis, Statistical theory of spot overlap for n-dimensional separations, Anal. Chem. 65 (1993) 2014–2023. doi:10.1021/ac00063a015.
D.R. Deans, A new technique for heart cutting in gas chromatography [1], Chromatographia 1 (1968) 18–22. doi:10.1007/BF02259005.
P. Dimitriou-Christidis, A. Bonvin, S. Samanipour, J. Hollender, R. Rutler, J. Westphale, J. Gros, J.S. Arey, GC×GC Quantification of priority and emerging nonpolar halogenated micropollutants in all types of wastewater matrices: analysis methodology, chemical occurrence, and partitioning, Environ. Sci. Technol. 49 (2015) 7914–7925. doi:10.1021/es5049122.
L.M. Dubois, K.A. Perrault, P.-H. Stefanuto, S. Koschinski, M. Edwards, L. McGregor, J.-F. Focant, Thermal desorption comprehensive two-dimensional gas chromatography coupled to variable-energy electron ionization time-of-flight mass spectrometry for monitoring subtle changes in volatile organic compound profiles of human blood, J. Chromatogr. A. 1501 (2017) 117–127. doi:10.1016/j.chroma.2017.04.026.
C. Duhamel, P. Cardinael, V. Peulon-Agasse, R. Firor, L. Pascaud, G. Semard-Jousset, P. Giusti, V. Livadaris, Comparison of cryogenic and differential flow (forward and reverse fill/flush) modulators and applications to the analysis of heavy petroleum cuts by high-temperature comprehensive gas chromatography, J. Chromatogr A. 1387 (2015) 95–103. doi:10.1016/j.chroma.2015.01.095.
M. Edwards, A. Mostafa, T. Górecki, Modulation in comprehensive two-dimensional gas chromatography: 20 years of innovation, Anal. Bioanal. Chem. 401 (2011) 2335–2349. doi:10.1007/s00216-011-5100-6.
C.E. Freye, B.D. Fitz, M.C. Billingsley, R.E. Synovec, Partial least squares analysis of rocket propulsion fuel data using diaphragm valve-based comprehensive two-dimensional gas chromatography coupled with flame ionization detection, Talanta 153 (2016) 203–210. doi:10.1016/j.talanta.2016.03.016.
C.E. Freye, R.E. Synovec, High temperature diaphragm valve-based comprehensive two-dimensional gas chromatography with time-of-flight mass spectrometry, Talanta 161 (2016) 675–680. doi:10.1016/j.talanta.2016.09.002.
C.E. Freye, H.D. Bahaghighat, R.E. Synovec, Comprehensive two-dimensional gas chromatography using partial modulation via a pulsed flow valve with a short modulation period, Talanta 177 (2018) 142–149. doi:10.1016/j.talanta.2017.08.095.
H.-J. de Geus, J. de Boer, U.A.T. Brinkman, Development of a thermal desorption modulator for gas chromatography, J. Chromatogr. A. 767 (1997) 137–151. doi:10.1016/S0021-9673(97)00038-1.
H.-J. de Geus, A. Schelvis, J. de Boer, U.A.Th. Brinkman, Comprehensive two-dimensional gas chromatography with a rotating thermal desorption modulator and independently temperature-programmable columns, J. High Res. Chromatogr. 23 (2000) 189–196. doi:10.1002/(SICI)1521-4168(20000301)23:3<189::AID-JHRC189>3.0.CO;2-N.
J.C. Giddings, Unified separation science, Wiley, New York, 1991. http://catalog.hathitrust.org/api/volumes/oclc/21764363.html.
D.V. Gough, H.D. Bahaghighat, R.E. Synovec, Column selection approach to achieve a high peak capacity in comprehensive three-dimensional gas chromatography, Talanta 195 (2019) 822–829. doi:10.1016/j.talanta.2018.12.007.

J.F. Griffith, W.L. Winniford, K. Sun, R. Edam, J.C. Luong, A reversed-flow differential flow modulator for comprehensive two-dimensional gas chromatography, J. Chromatogr. A. 1226 (2012) 116–123. doi:10.1016/j.chroma.2011.11.036.
J. Harynuk, T. Górecki, Comprehensive two-dimensional gas chromatography in stop-flow mode, J. Sep. Sci. 27 (2004) 431–441. doi:10.1002/jssc.200301649.
W. Khummueng, J. Harynuk, P.J. Marriott, Modulation ratio in comprehensive two-dimensional gas chromatography, Anal. Chem. 78 (2006) 4578–4587. doi:10.1021/ac052270b.
M.S. Klee, GC inlets an introduction, second, Agilent Technologies, Inc., Wilmington, DE USA, 2005. http://www.agilent.com/cs/library/usermanuals/public/5958-9468_041007.pdf.
M.S. Klee, J. Cochran, M. Merrick, L.M. Blumberg, Evaluation of conditions of comprehensive two-dimensional gas chromatography that yield a near-theoretical maximum in peak capacity gain, J. Chromatogr A. 1383 (2015) 151–159. doi:10.1016/j.chroma.2015.01.031.
E.B. Ledford, C. Billesbach, Jet-cooled thermal modulator for comprehensive multidimensional gas chromatography, J. High Resolut. Chromatogr. 23 (2000) 202–204. doi:10.1002/(SICI)1521-4168(20000301)23:3<202::AID-JHRC202>3.0.CO;2-5.
Z. Liu, J.B. Phillips, Comprehensive two-dimensional gas chromatography using an on-column thermal modulator interface, J. Chromatogr. Sci. 29 (1991) 227–231. doi:10.1093/chromsci/29.6.227.
L. Mahé, M. Courtiade, C. Dartiguelongue, J. Ponthus, V. Souchon, D. Thiébaut, Overcoming the high-temperature two-dimensional gas chromatography limits to elute heavy compounds, J. Chromatogr. A. 1229 (2012) 298–301. doi:10.1016/j.chroma.2012.01.030.
P.J. Marriott, R.M. Kinghorn, Longitudinally modulated cryogenic system. A generally applicable approach to solute trapping and mobilization in gas chromatography, Anal. Chem. 69 (1997) 2582–2588. doi:10.1021/ac961310w.
D. Megson, R. Kalin, P.J. Worsfold, C. Gauchotte-Lindsay, D.G. Patterson, M.C. Lohan, S. Comber, T.A. Brown, G. O'Sullivan, Fingerprinting polychlorinated biphenyls in environmental samples using comprehensive two-dimensional gas chromatography with time-of-flight mass spectrometry, J. Chromatogr. A. 1318 (2013) 276–283. doi:10.1016/j.chroma.2013.10.016.
A.M. Muscalu, M. Edwards, T. Górecki, E.J. Reiner, Evaluation of a single-stage consumable-free modulator for comprehensive two-dimensional gas chromatography: Analysis of polychlorinated biphenyls, organochlorine pesticides and chlorobenzenes, J. Chromatogr. A. 1391 (2015) 93–101. doi:10.1016/j.chroma.2015.02.074.
B.A. Parsons, D.K. Pinkerton, R.E. Synovec, Implications of phase ratio for maximizing peak capacity in comprehensive two-dimensional gas chromatography time-of-flight mass spectrometry, J. Chromatogr. A 1536 (2018) 16–26. doi:10.1016/j.chroma.2017.07.018.
J.B. Phillips, J. Xu, Comprehensive multi-dimensional gas chromatography, J. Chromatogr. A. 703 (1995) 327–334. doi:10.1016/0021-9673(95)00297-Z.
J.B. Phillips, E.B. Ledford, Thermal modulation: A chemical instrumentation component of potential value in improving portability, Field Anal. Chem. Technol. 1 (1996) 23–29. doi:10.1002/(SICI)1520-6521(1996)1:1<23::AID-FACT4>3.0.CO;2-F.
J.B. Phillips, R.B. Gaines, J. Blomberg, F.W.M. van der Wielen, J.-M. Dimandja, V. Green, J. Granger, D. Patterson, L. Racovalis, H.-J. de Geus, J. de Boer, P. Haglund, J. Lipsky, V. Sinha, E.B. Ledford, A robust thermal modulator for comprehensive two-dimensional gas chromatography, J. High Resolut. Chromatogr. 22 (1999) 3–10. doi:10.1002/(SICI)1521-4168(19990101)22:1<3::AID-JHRC3>3.0.CO;2-U.

S. Prebihalo, A. Brockman, J. Cochran, F.L. Dorman, Determination of emerging contaminants in wastewater utilizing comprehensive two-dimensional gas-chromatography coupled with time-of-flight mass spectrometry, J. Chromatogr. A. 1419 (2015) 109–115. doi:10.1016/j.chroma.2015.09.080.
S.E. Prebihalo, K.L. Berrier, C.E. Freye, H.D. Bahaghighat, N.R. Moore, D.K. Pinkerton, R.E. Synovec, Multidimensional gas chromatography: advances in instrumentation, chemometrics, and applications, Anal. Chem. (2017). doi:10.1021/acs.analchem.7b04226.
J.V. Seeley, F. Kramp, C.J. Hicks, Comprehensive two-dimensional gas chromatography via differential flow modulation, Anal. Chem. 72 (2000) 4346–4352. doi:10.1021/ac000249z.
J.V. Seeley, Theoretical study of incomplete sampling of the first dimension in comprehensive two-dimensional chromatography, J. Chromatogr A. 962 (2002) 21–27. doi:10.1016/S0021-9673(02)00461-2.
J.V. Seeley, N.J. Micyus, S.V. Bandurski, S.K. Seeley, J.D. McCurry, Microfluidic deans switch for comprehensive two-dimensional gas chromatography, Anal. Chem. 79 (2007) 1840–1847. doi:10.1021/ac061881g.
J.V. Seeley, Recent advances in flow-controlled multidimensional gas chromatography, J. Chromatogr A. 1255 (2012) 24–37. doi:10.1016/j.chroma.2012.01.027.
J.V. Seeley, N.E. Schimmel, S.K. Seeley, The multi-mode modulator: A versatile fluidic device for two-dimensional gas chromatography, J. Chromatogr. A. 1536 (2018) 6–15. doi:10.1016/j.chroma.2017.06.030.
W.C. Siegler, J.A. Crank, D.W. Armstrong, R.E. Synovec, Increasing selectivity in comprehensive three-dimensional gas chromatography via an ionic liquid stationary phase column in one dimension, J. Chromatogr. A. 1217 (2010) 3144–3149. doi:10.1016/j.chroma.2010.02.082.
W.C. Siegler, B.D. Fitz, J.C. Hoggard, R.E. Synovec, Experimental study of the quantitative precision for valve-based comprehensive two-dimensional gas chromatography, Anal. Chem. 83 (2011) 5190–5196. doi:10.1021/ac200302b.
P.-H. Stefanuto, K.A. Perrault, L.M. Dubois, B. L'Homme, C. Allen, C. Loughnane, N. Ochiai, J.-F. Focant, Advanced method optimization for volatile aroma profiling of beer using two-dimensional gas chromatography time-of-flight mass spectrometry, J. Chromatogr. A. 1507 (2017) 45–52. doi:10.1016/j.chroma.2017.05.064.
D.R. Stoll, X. Wang, P.W. Carr, Comparison of the practical resolving power of one- and two-dimensional high-performance liquid chromatography analysis of metabolomic samples, Anal. Chem. 80 (2008) 268–278. doi:10.1021/ac701676b.
N.E. Watson, W.C. Siegler, J.C. Hoggard, R.E. Synovec, Comprehensive three-dimensional gas chromatography with parallel factor analysis, Anal. Chem. 79 (2007) 8270–8280. doi:10.1021/ac070829x.
N.E. Watson, H.D. Bahaghighat, K. Cui, R.E. Synovec, Comprehensive three-dimensional gas chromatography with time-of-flight mass spectrometry, Anal. Chem. 89 (2017) 1793–1800. doi:10.1021/acs.analchem.6b04112.
N.E. Watson, S.E. Prebihalo, R.E. Synovec, Targeted analyte deconvolution and identification by four-way parallel factor analysis using three-dimensional gas chromatography with mass spectrometry data, Anal. Chim. Acta (2017). doi:10.1016/j.aca.2017.06.017.
J.E. Welke, V. Manfroi, M. Zanus, M. Lazzarotto, C. Alcaraz Zini, Differentiation of wines according to grape variety using multivariate analysis of comprehensive two-dimensional

gas chromatography with time-of-flight mass spectrometric detection data, Food Chem. 141 (2013) 3897–3905. doi:10.1016/j.foodchem.2013.06.100.